Supporting Information

Solid State Tuning of TiO_2 Morphology, Crystal Phase and Size through Metal Macromolecular Complexes and its Significance in the Photocatalytic Response

Patricio Allende Gonzalez[1], Miguel Ángel Laguna-Bercero[2], Lorena Barrientos*[3], María Luisa Valenzuela[4] and Carlos Díaz*[1]

*1. Departamento de Química, Facultad de Ciencias, Universidad de Chile. La Palmeras 3425, Ñuñoa, casilla 653, Santiago de Chile, 7800003, Chile. *Corresponding author E-mail: cdiaz@uchile.cl*

2. Instituto de Ciencia de Materiales de Aragón, ICMA, CSIC-Universidad de Zaragoza, María de Luna 3, 50018 – Zaragoza, Spain.

*3. Facultad de Química, Centro de Investigación en Nanotecnología y Materiales Avanzados CIEN-UC, Pontificia Universidad Católica de Chile, Vicuña Mackenna 4860, Macul, Santiago de Chile, Chile. *Corresponding author E-mail: lbarrientop@uc.cl*

4. Universidad Autónoma de Chile, Institute of Applied Chemical Sciences, Inorganic Chemistry and Molecular Materials Group, El Llano Subercaseaux 2801, 5° piso, San Miguel, Santiago, Chile.

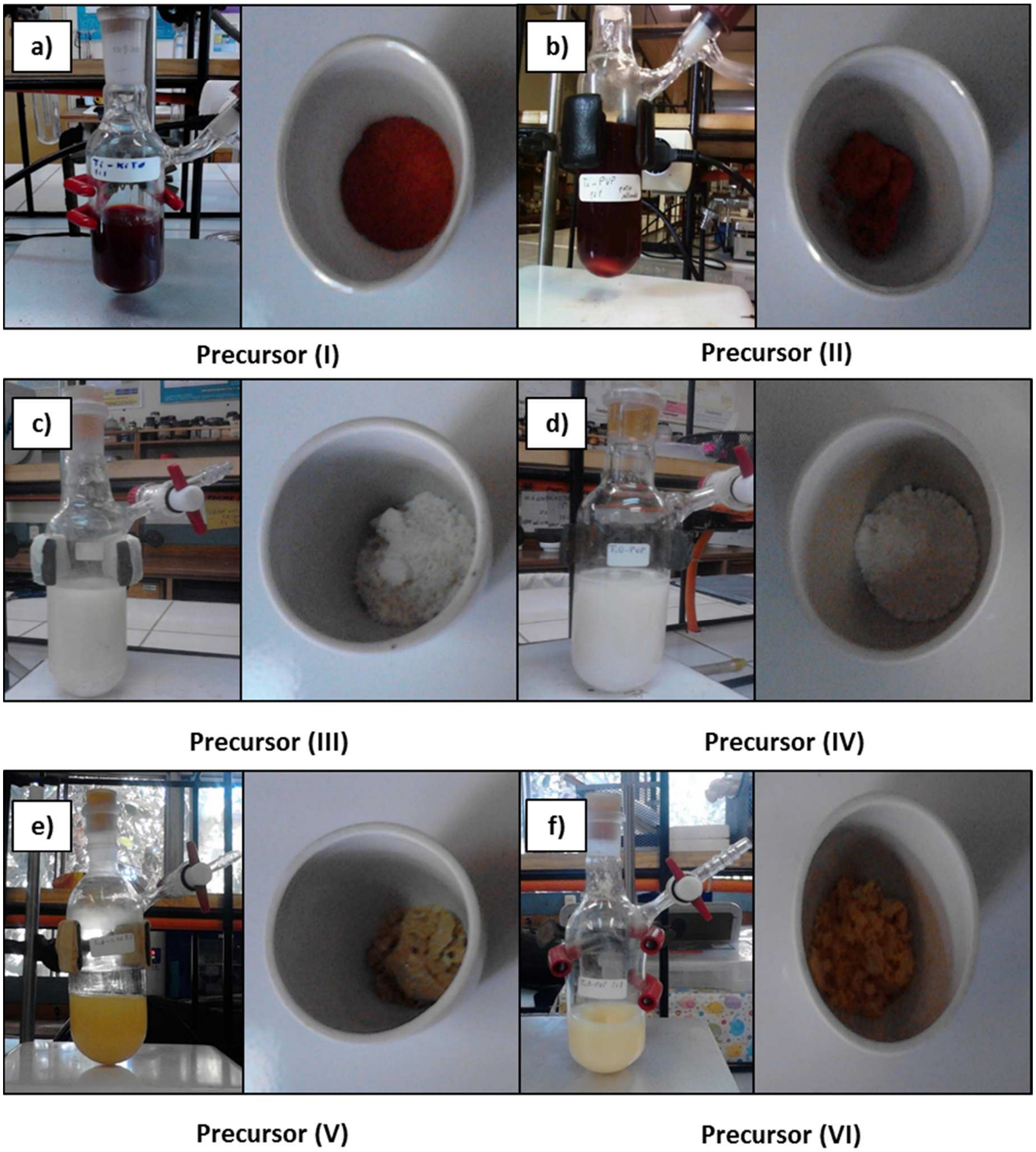

Figure S1. Images of synthesized solid precursors; (a) Chitosan·(Cp_2TiCl_2), (b) PS-co-4-PVP·(Cp_2TiCl_2), (c) Chitosan·($TiOSO_4$), (d) PS-co-4-PVP·($TiOSO_4$), (e) Chitosan·$TiO(acac)_2$ and (f) PS-co-4-PVP·$TiO(acac)_2$.

(a)

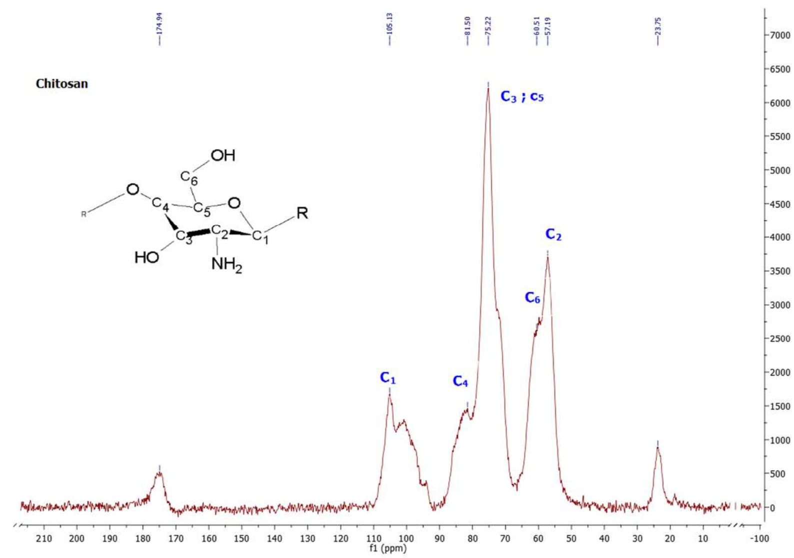
Chitosan
174.94
105.13
81.50
75.22
60.51
57.19
23.75
C3 ; c5
C2
C6
C1
C4
OH
C6
O
C4
C5
O
R
C3
C2
C1
HO
NH2
f1 (ppm)

(b)

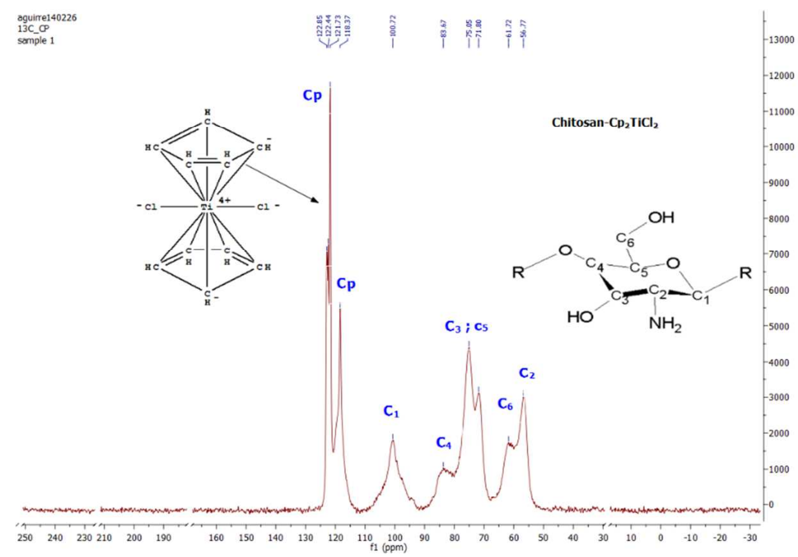
aguirre140226
13C_CP
sample 1
122.85
122.44
121.73
118.37
100.72
83.67
75.05
71.80
61.72
56.77
Cp
Cp
Chitosan-Cp2TiCl2
Ti
4+
Cl
Cl
C3 ; c5
C2
C6
C1
C4
OH
NH2
HO
R
f1 (ppm)

(c)

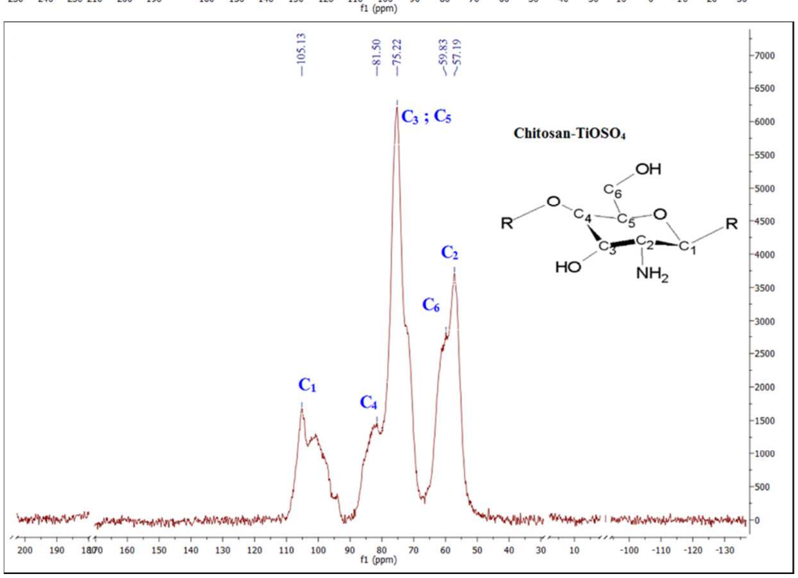
105.13
81.50
75.22
59.83
57.19
C3 ; C5
Chitosan-TiOSO4
C2
C6
C1
C4
OH
NH2
HO
R
f1 (ppm)

(d)

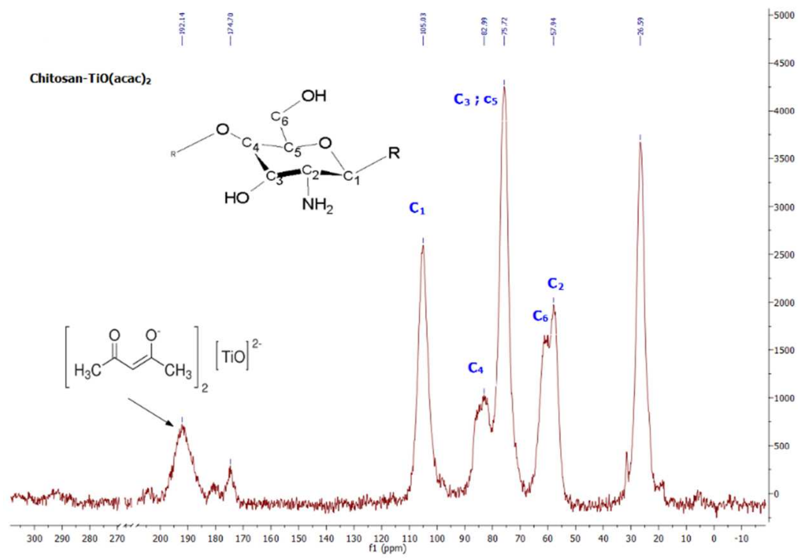

Chitosan-TiO(acac)2
192.14
174.70
105.03
82.99
75.72
57.94
26.59
C3 ; c5
C1
C4
C6
C2
OH
NH2
HO
R
[TiO]2-
H3C
CH3
f1 (ppm)

(e)

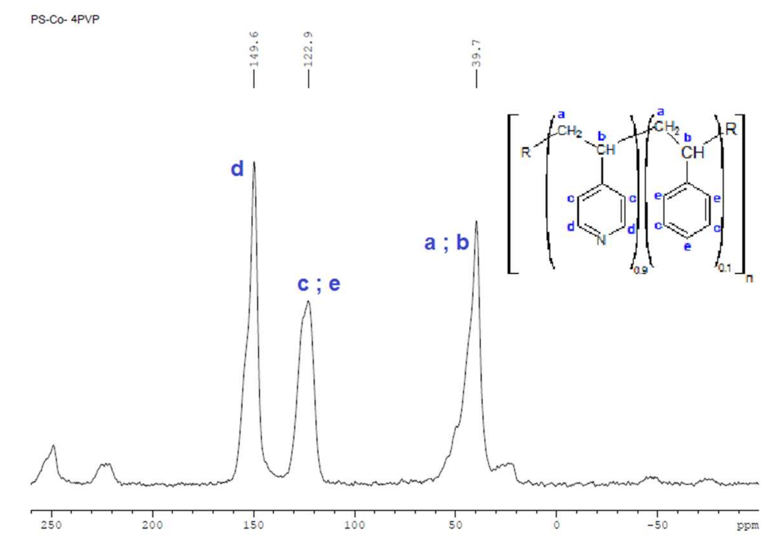

PS-Co- 4PVP
149.6
122.9
39.7
d
c ; e
a ; b
ppm

(f)

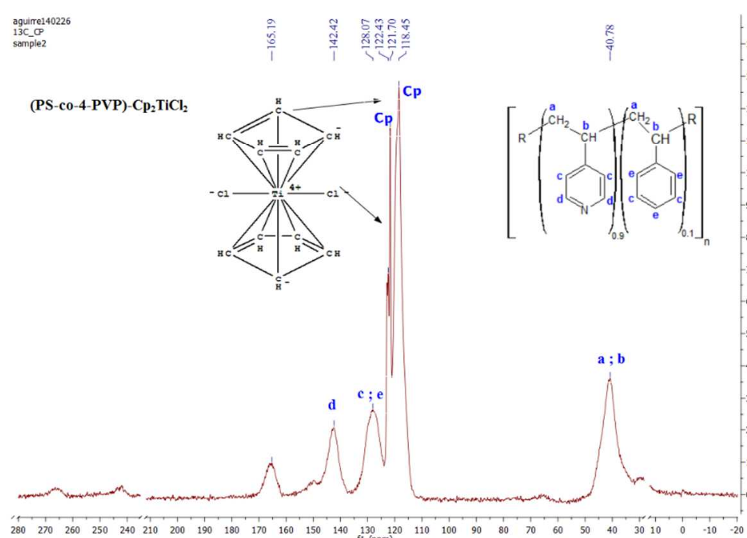

aguirre140226
13C_CP
sample2
(PS-co-4-PVP)-Cp2TiCl2
165.19
142.42
128.07
122.43
121.70
118.45
40.78
Cp
Cp
d
c ; e
a ; b
f1 (ppm)

(g)

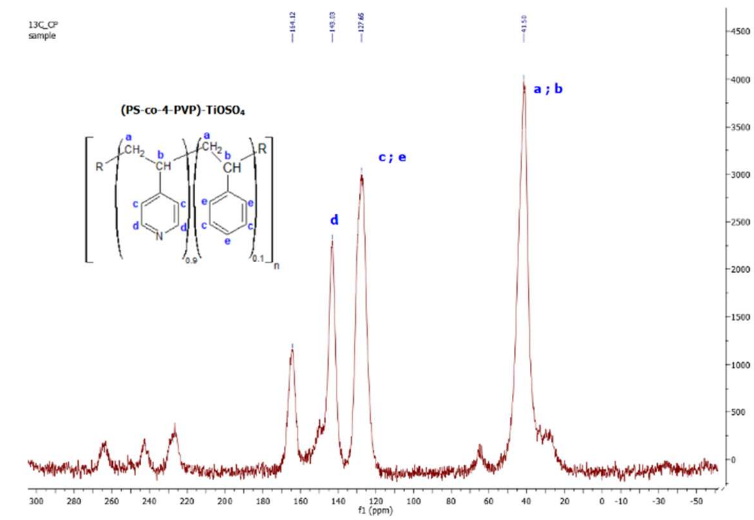

(h)

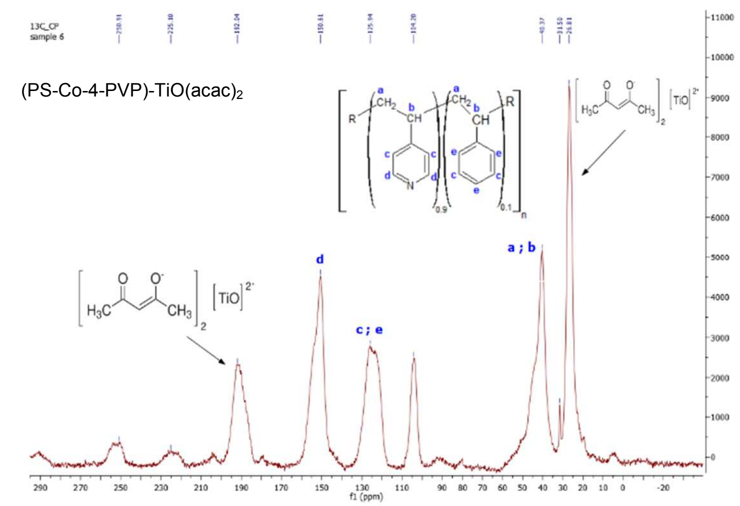

Figure S2. ^{13}C MAS NMR spectra of all macromolecular complexes and pure polymers. (a) pure chitosan, (b) chitosan-Cp_2TiCl_2, (c) chitosan-$TiOSO_4$, (d) chitosan-$TiO(acac)_2$, (e) pure PS-Co-4-PVP, (f) (PS-Co-4-PVP)-Cp_2TiCl_2, (g) (PS-Co-4-PVP)-$TiOSO_4$ and (h) (PS-Co-4-PVP)-$TiO(acac)_2$.

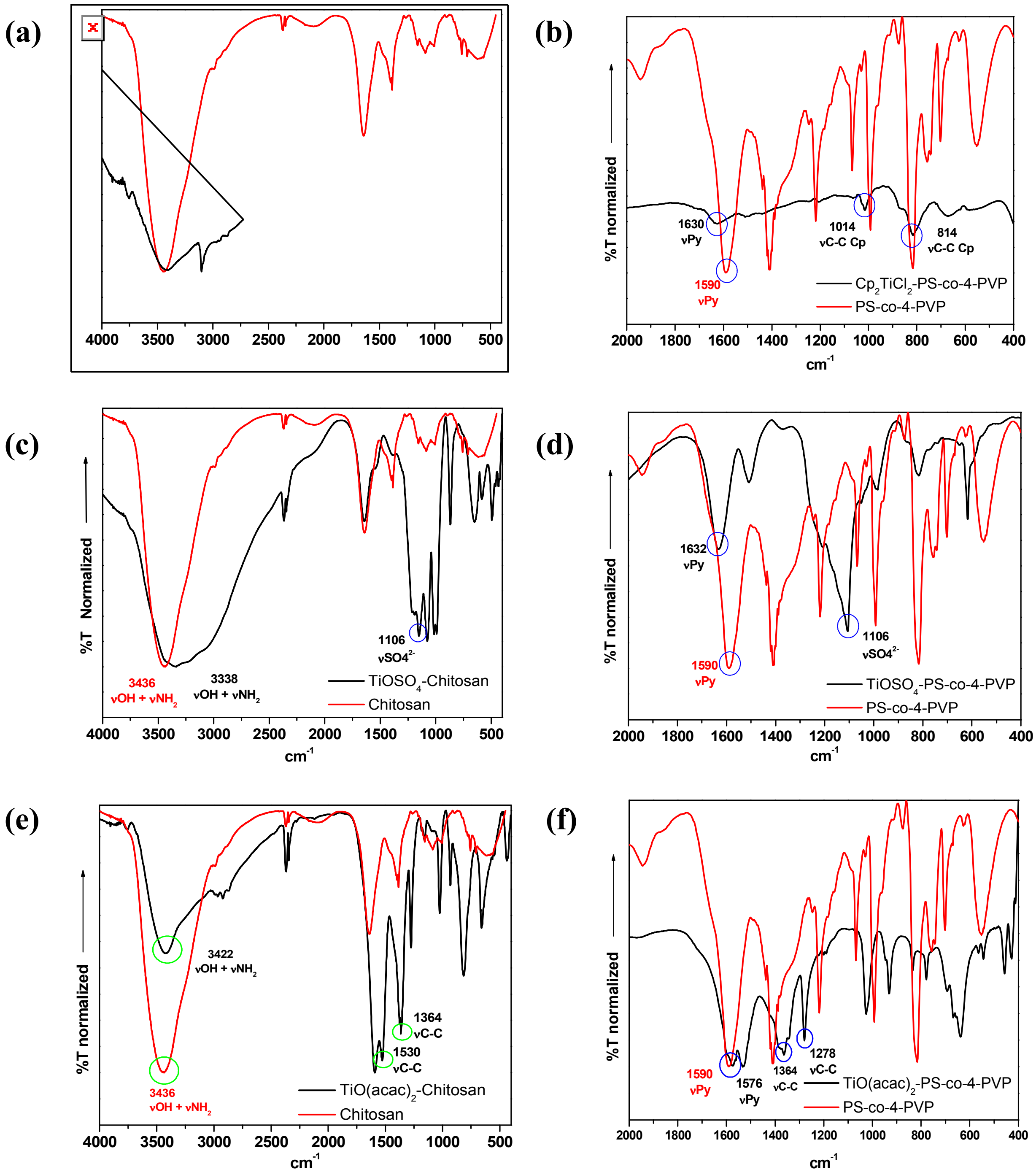

Figure S3. IR spectra of macromolecular complexes (black line) in comparison to pure polymers (red line), showing the shifting signals assigned to the complex formation. (a) chitosan-Cp_2TiCl_2, (b) (PS-Co-4-PVP)-Cp_2TiCl_2, (c) chitosan-$TiOSO_4$, (d) (PS-Co-4-PVP)-$TiOSO_4$, (e) chitosan-$TiO(acac)_2$ and (f) (PS-Co-4-PVP)-$TiO(acac)_2$.

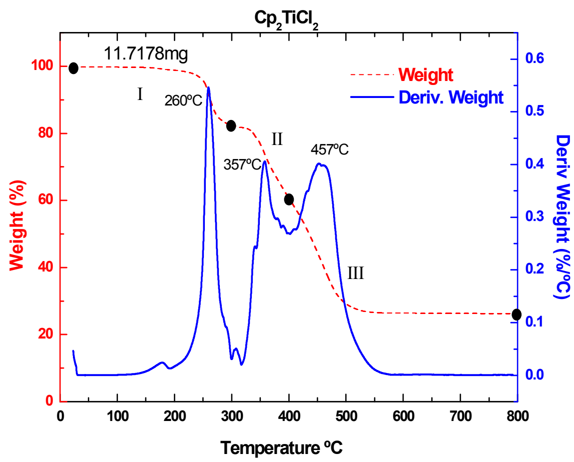
Cp2TiCl2
11.7178mg
Weight
Deriv. Weight
260ºC
357ºC
457ºC
I
II
III
Weight (%)
Deriv Weight (%/ºC)
Temperature ºC

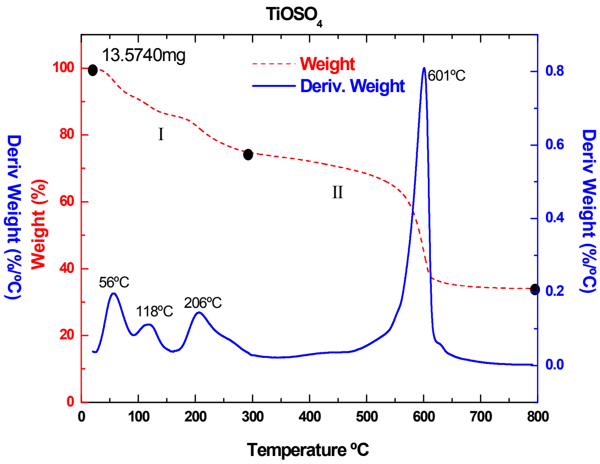
TiOSO4
13.5740mg
Weight
Deriv. Weight
601ºC
56ºC
118ºC
206ºC
I
II
Weight (%)
Deriv Weight (%/ºC)
Temperature ºC

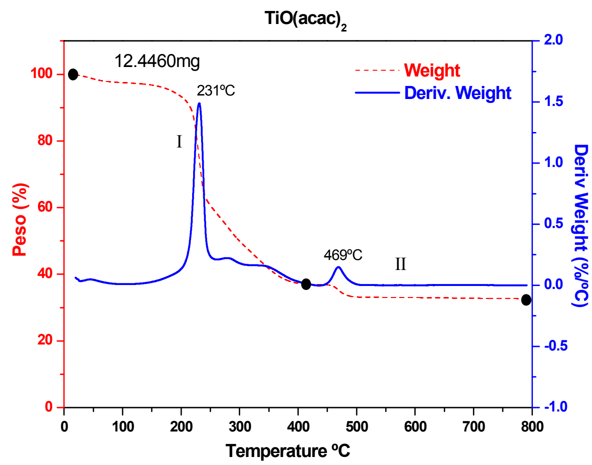
TiO(acac)2
12.4460mg
Weight
Deriv. Weight
231ºC
469ºC
I
II
Peso (%)
Deriv Weight (%/ºC)
Temperature ºC

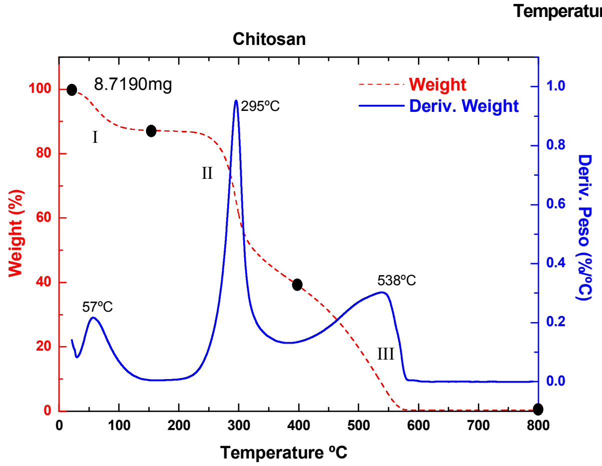
Chitosan
8.7190mg
Weight
Deriv. Weight
295ºC
57ºC
538ºC
I
II
III
Weight (%)
Deriv. Peso (%/ºC)
Temperature ºC

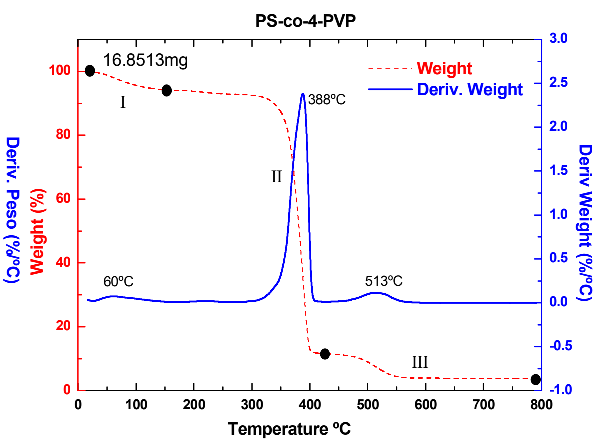
PS-co-4-PVP
16.8513mg
Weight
Deriv. Weight
388ºC
60ºC
513ºC
I
II
III
Weight (%)
Deriv Weight (%/ºC)
Temperature ºC

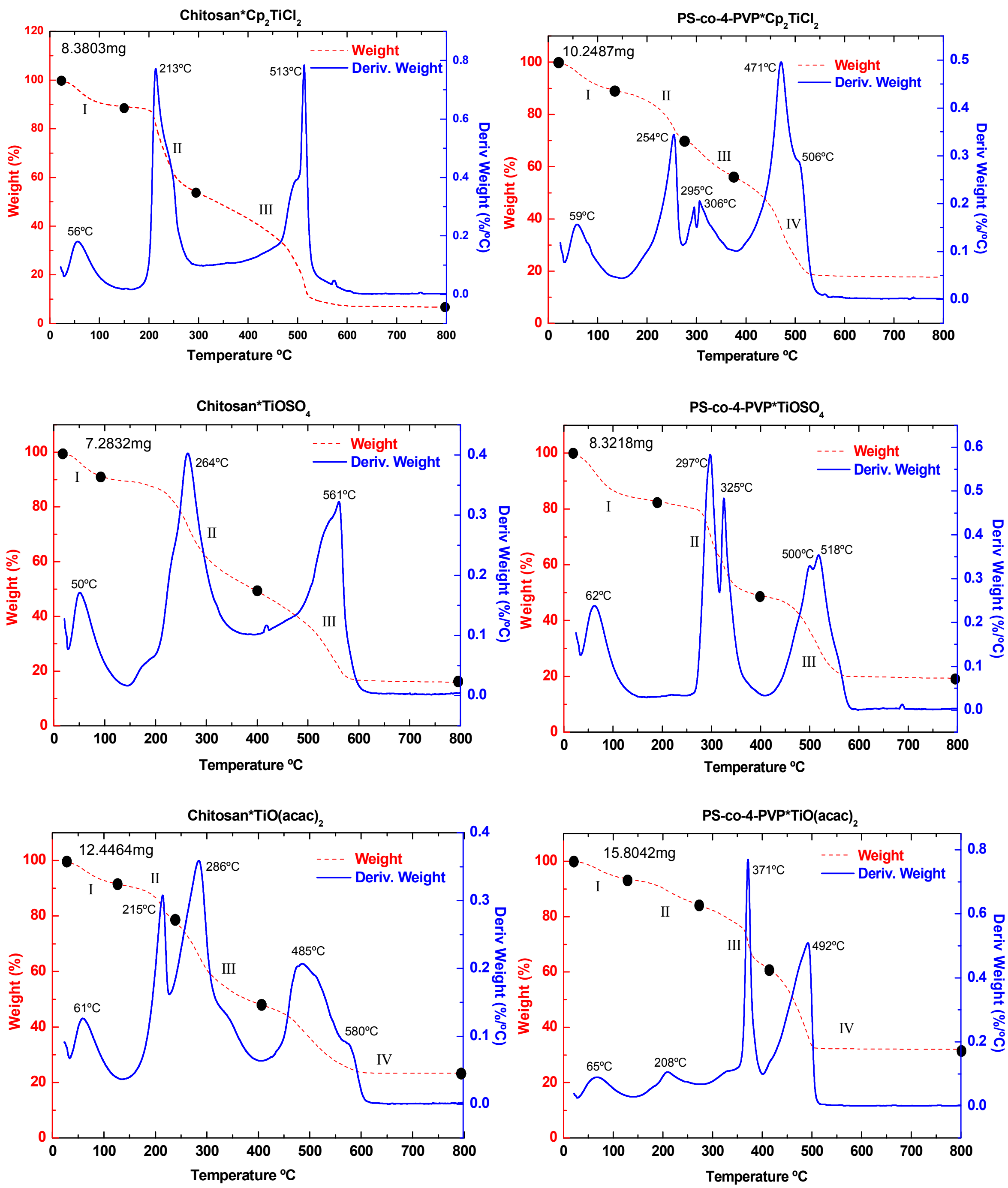

Figure S4. TG/DTA curves of macromolecular complexes.

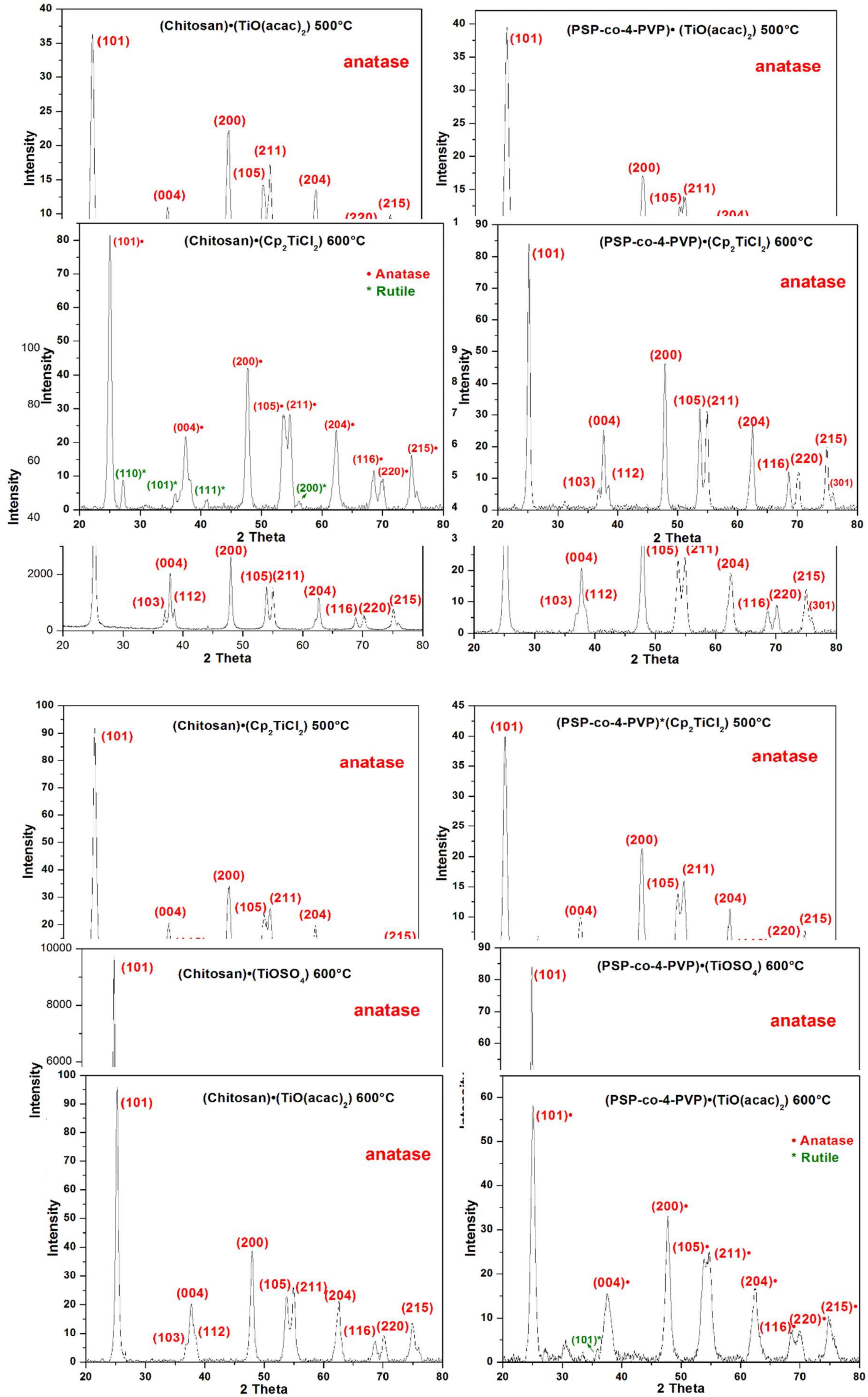

(Chitosan)•(TiO(acac)$_2$) 500°C
anatase
(PSP-co-4-PVP)• (TiO(acac)$_2$) 500°C
anatase
(Chitosan)•(Cp$_2$TiCl$_2$) 600°C
• Anatase
* Rutile
(PSP-co-4-PVP)•(Cp$_2$TiCl$_2$) 600°C
anatase
(Chitosan)•(Cp$_2$TiCl$_2$) 500°C
anatase
(PSP-co-4-PVP)*(Cp$_2$TiCl$_2$) 500°C
anatase
(Chitosan)•(TiOSO$_4$) 600°C
anatase
(PSP-co-4-PVP)•(TiOSO$_4$) 600°C
anatase
(Chitosan)•(TiO(acac)$_2$) 600°C
anatase
(PSP-co-4-PVP)•(TiO(acac)$_2$) 600°C
• Anatase
* Rutile
Intensity
2 Theta

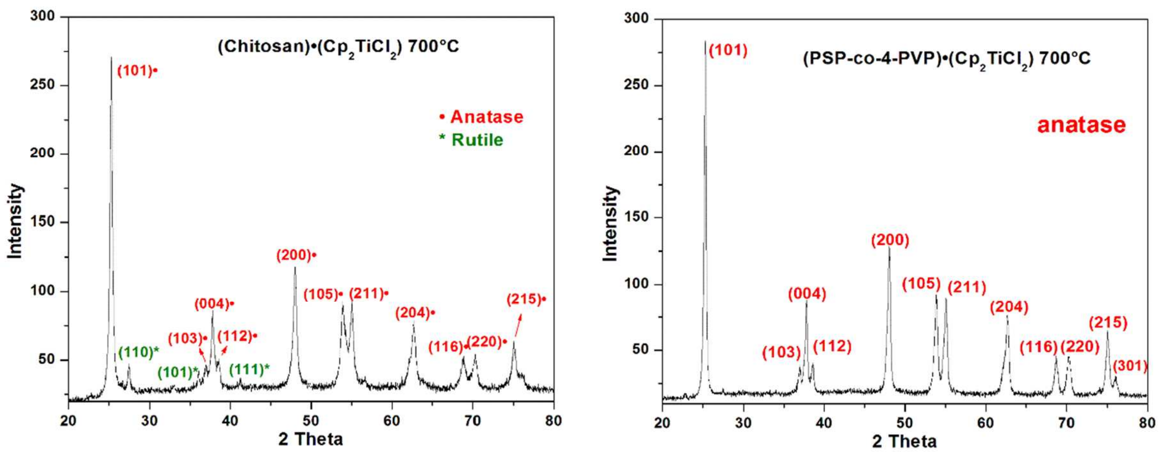

Figure S5. PXRD patterns for pyrolytic products from precursors (I)-(VI) at 500, 600, 700,

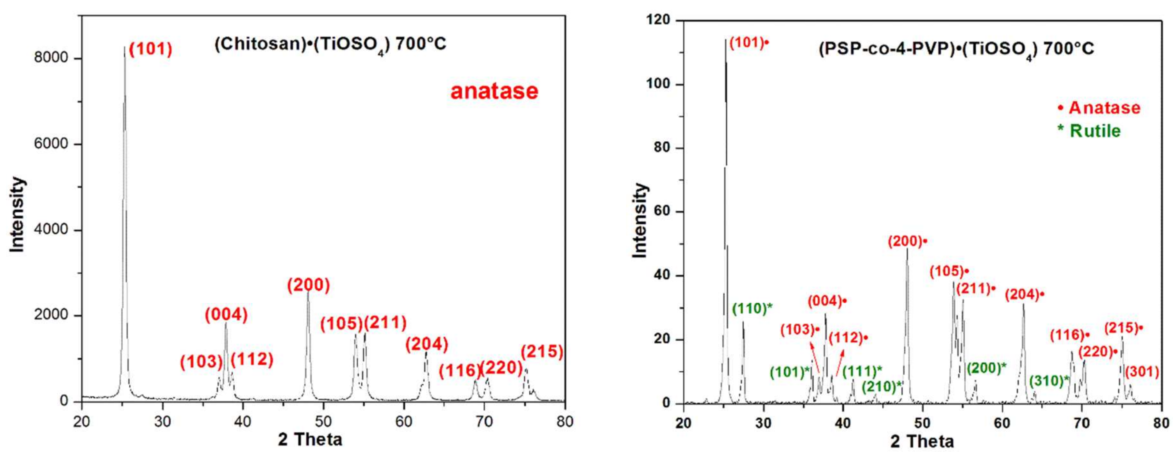

800°C.

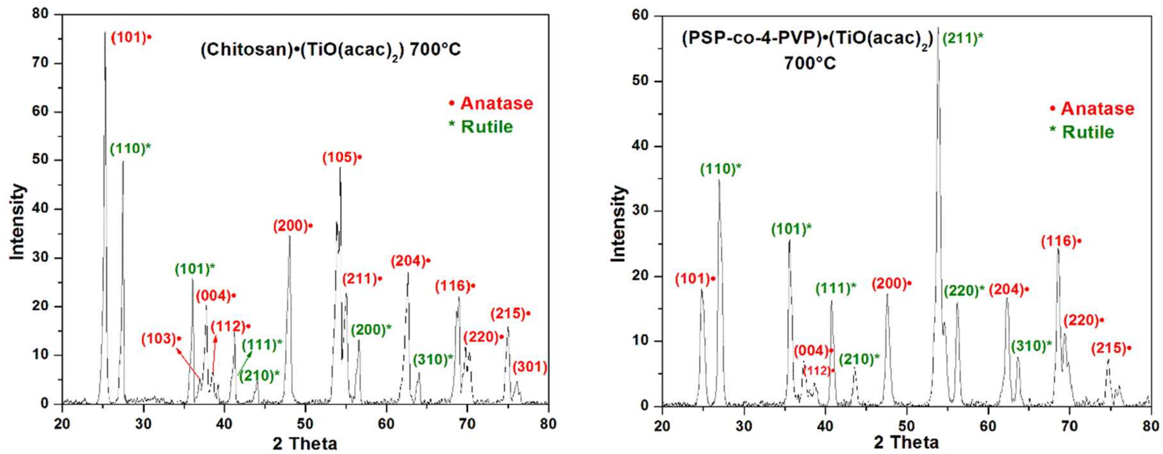

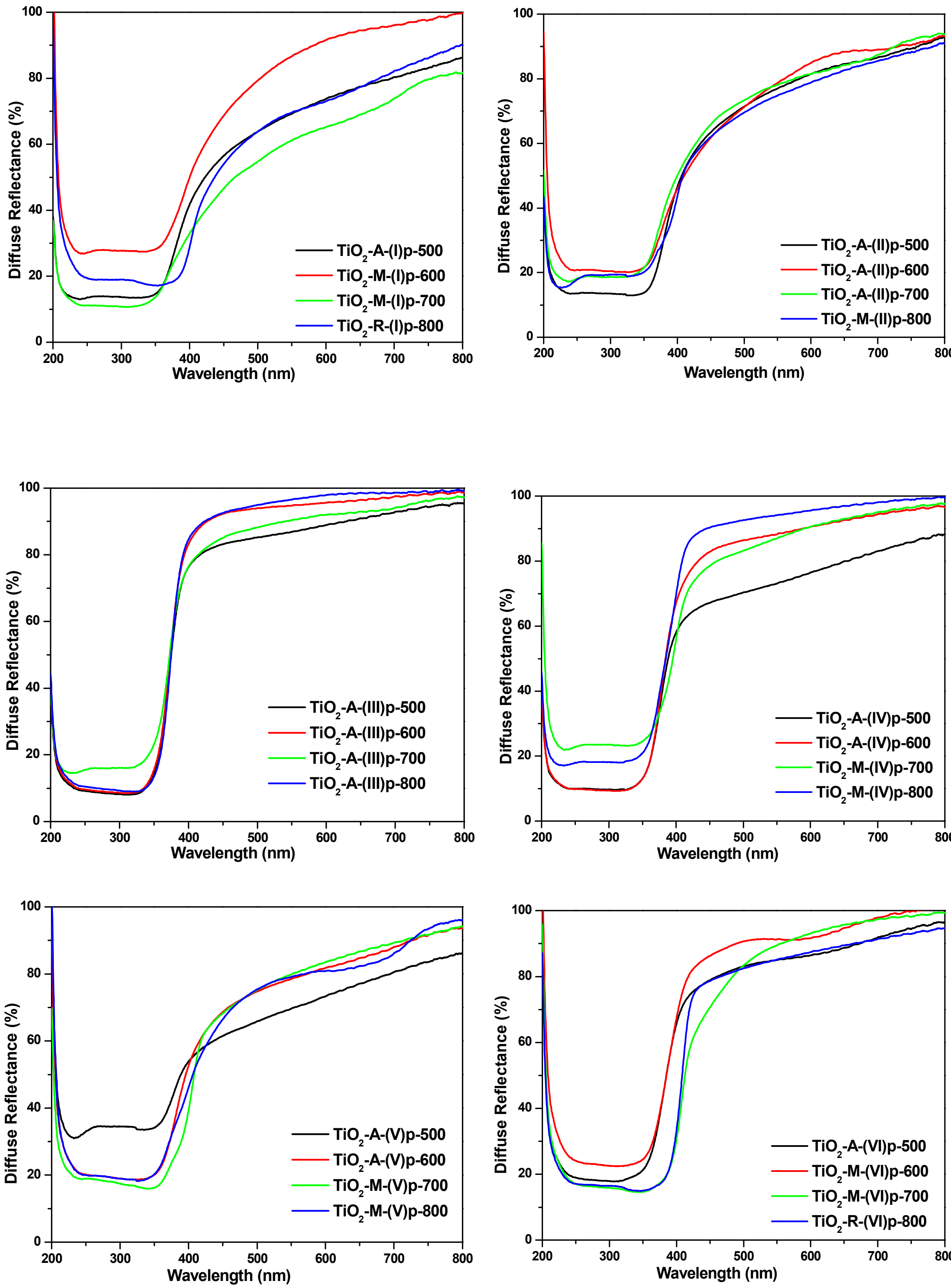

Figure S6. Diffuse Reflectance from different TiO_2 nanostructures

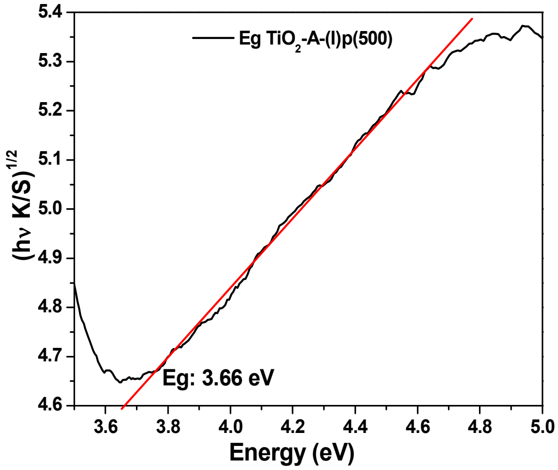
Eg TiO2-A-(I)p(500)
Eg: 3.66 eV
(hν K/S)1/2
Energy (eV)

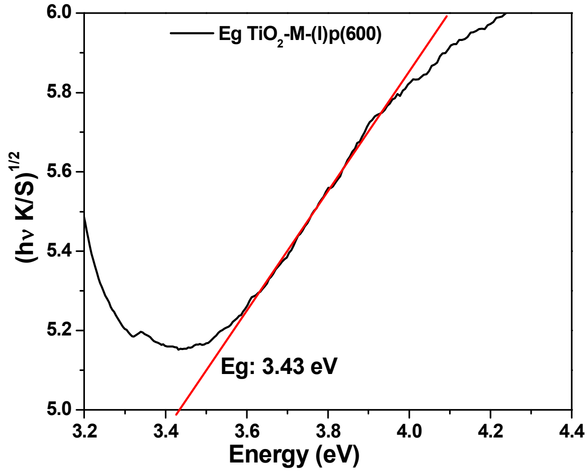
Eg TiO2-M-(I)p(600)
Eg: 3.43 eV
(hν K/S)1/2
Energy (eV)

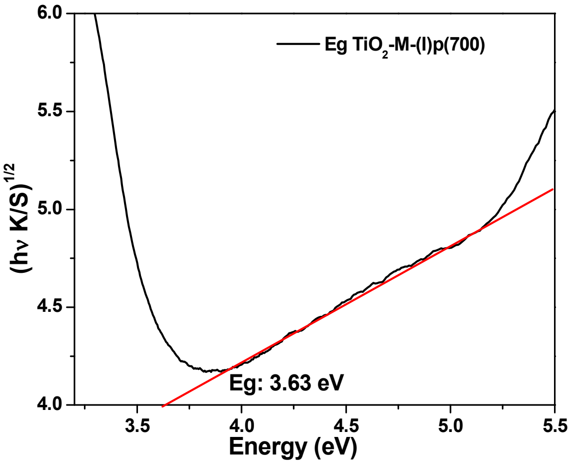
Eg TiO2-M-(I)p(700)
Eg: 3.63 eV
(hν K/S)1/2
Energy (eV)

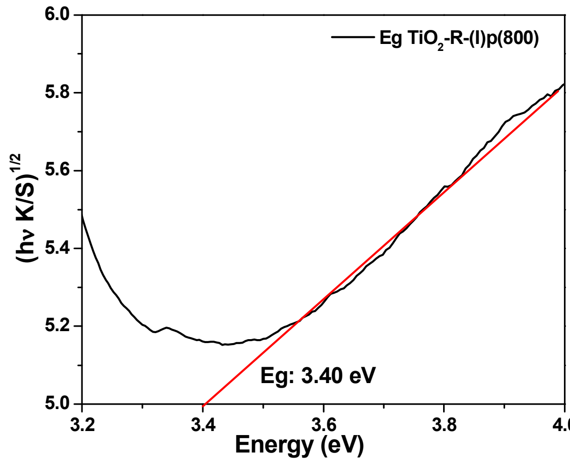
Eg TiO2-R-(I)p(800)
Eg: 3.40 eV
(hν K/S)1/2
Energy (eV)

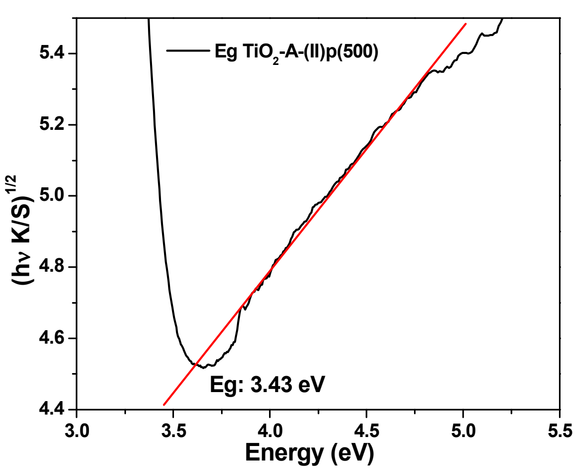
Eg TiO2-A-(II)p(500)
Eg: 3.43 eV
(hν K/S)1/2
Energy (eV)

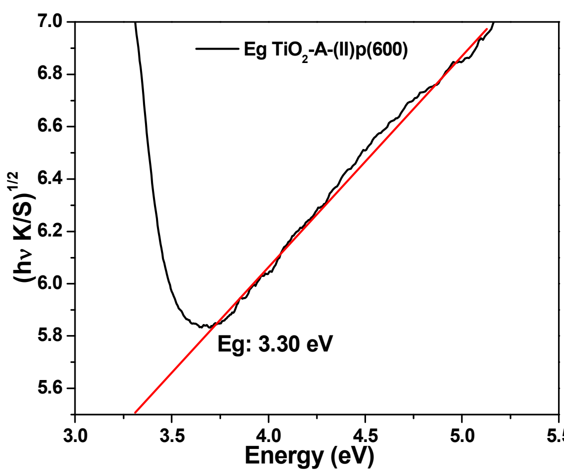
Eg TiO2-A-(II)p(600)
Eg: 3.30 eV
(hν K/S)1/2
Energy (eV)

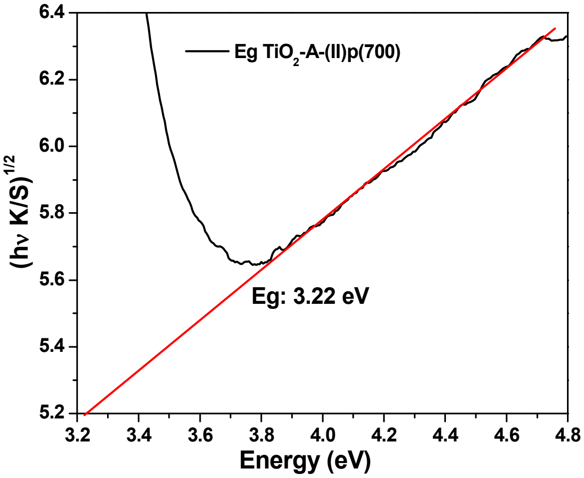
Eg TiO_2-A-(II)p(700)
Eg: 3.22 eV
$(h\nu\ K/S)^{1/2}$
Energy (eV)
5.2 5.4 5.6 5.8 6.0 6.2 6.4
3.2 3.4 3.6 3.8 4.0 4.2 4.4 4.6 4.8

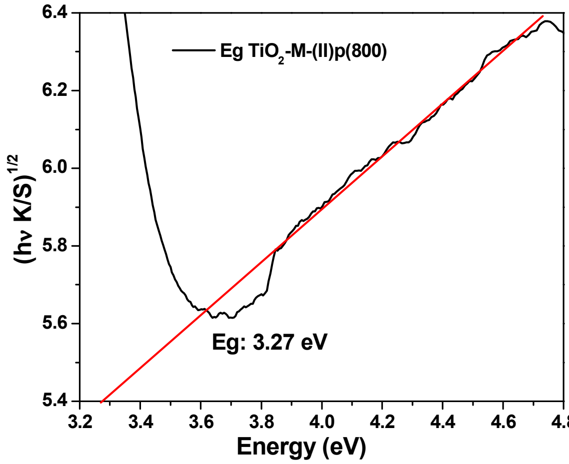
Eg TiO_2-M-(II)p(800)
Eg: 3.27 eV
$(h\nu\ K/S)^{1/2}$
Energy (eV)
5.4 5.6 5.8 6.0 6.2 6.4
3.2 3.4 3.6 3.8 4.0 4.2 4.4 4.6 4.8

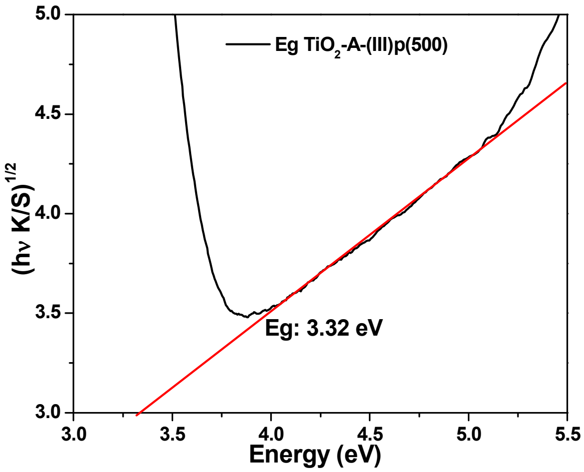
Eg TiO_2-A-(III)p(500)
Eg: 3.32 eV
$(h\nu\ K/S)^{1/2}$
Energy (eV)
3.0 3.5 4.0 4.5 5.0
3.0 3.5 4.0 4.5 5.0 5.5

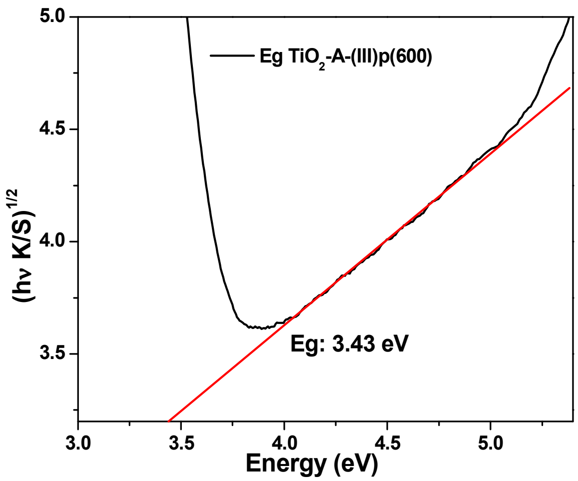
Eg TiO_2-A-(III)p(600)
Eg: 3.43 eV
$(h\nu\ K/S)^{1/2}$
Energy (eV)
3.5 4.0 4.5 5.0
3.0 3.5 4.0 4.5 5.0

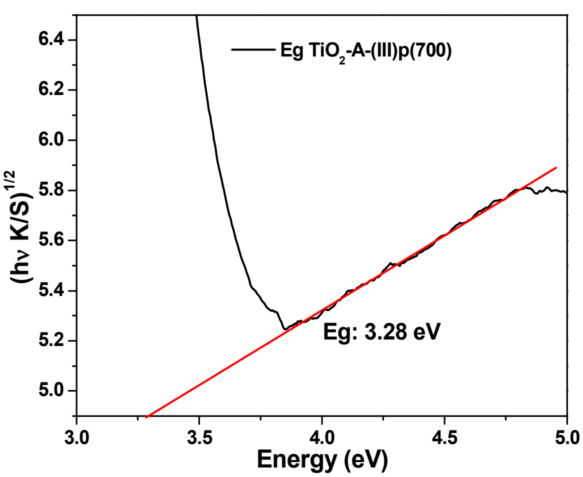
Eg TiO_2-A-(III)p(700)
Eg: 3.28 eV
$(h\nu\ K/S)^{1/2}$
Energy (eV)
5.0 5.2 5.4 5.6 5.8 6.0 6.2 6.4
3.0 3.5 4.0 4.5 5.0

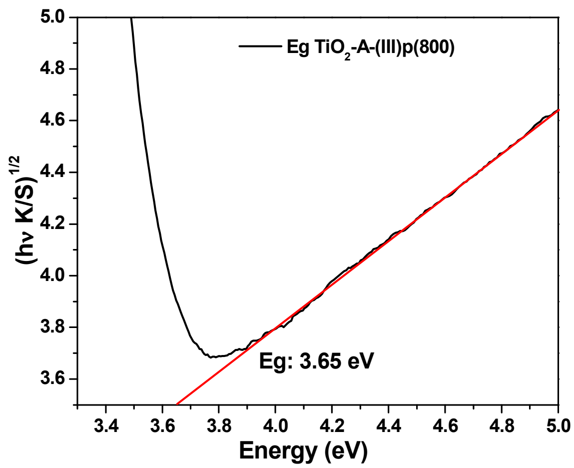
Eg TiO_2-A-(III)p(800)
Eg: 3.65 eV
$(h\nu\ K/S)^{1/2}$
Energy (eV)
3.6 3.8 4.0 4.2 4.4 4.6 4.8 5.0
3.4 3.6 3.8 4.0 4.2 4.4 4.6 4.8 5.0

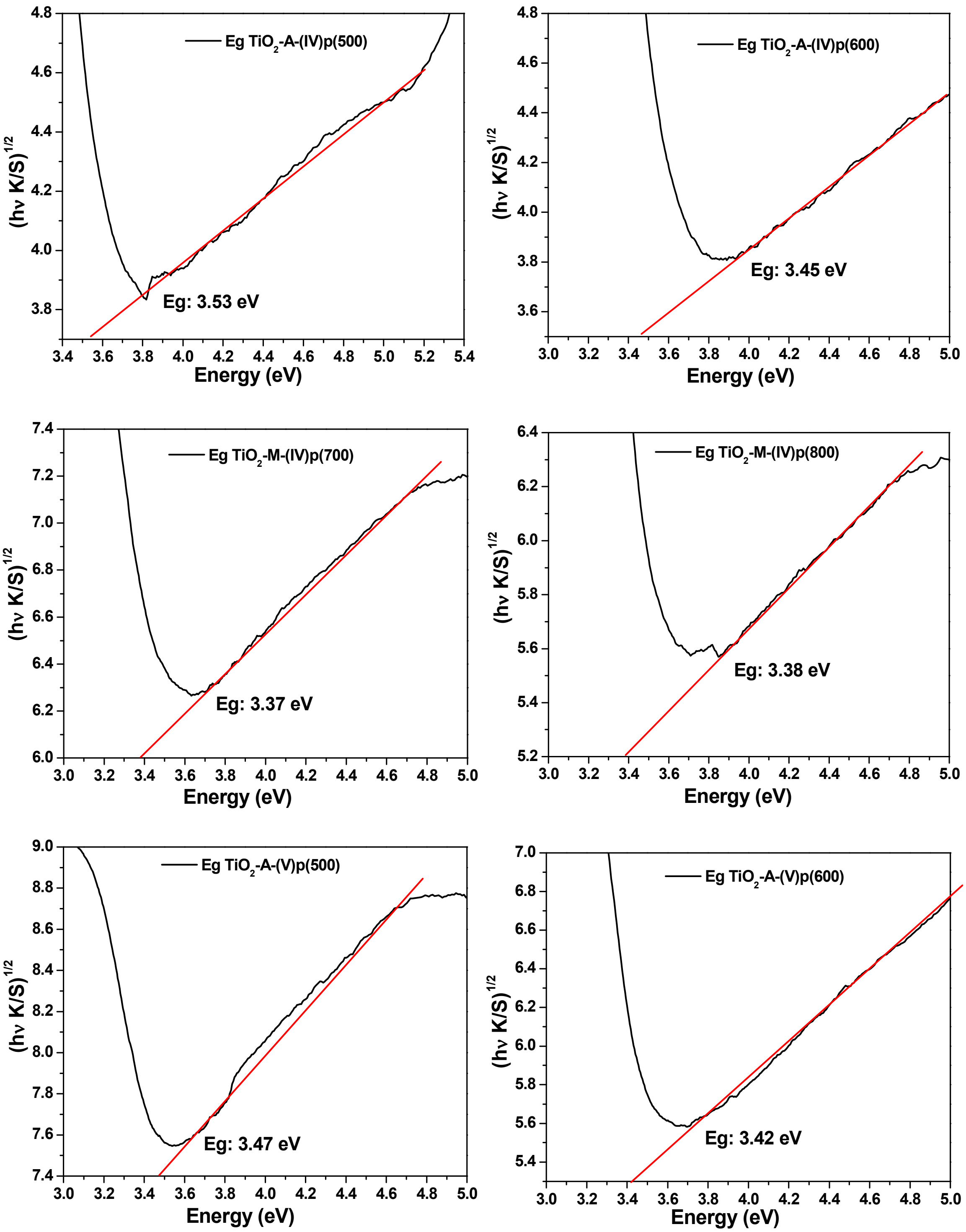

Eg TiO2-A-(IV)p(500)
Eg: 3.53 eV
Eg TiO2-A-(IV)p(600)
Eg: 3.45 eV
Eg TiO2-M-(IV)p(700)
Eg: 3.37 eV
Eg TiO2-M-(IV)p(800)
Eg: 3.38 eV
Eg TiO2-A-(V)p(500)
Eg: 3.47 eV
Eg TiO2-A-(V)p(600)
Eg: 3.42 eV
(hν K/S)^1/2
Energy (eV)

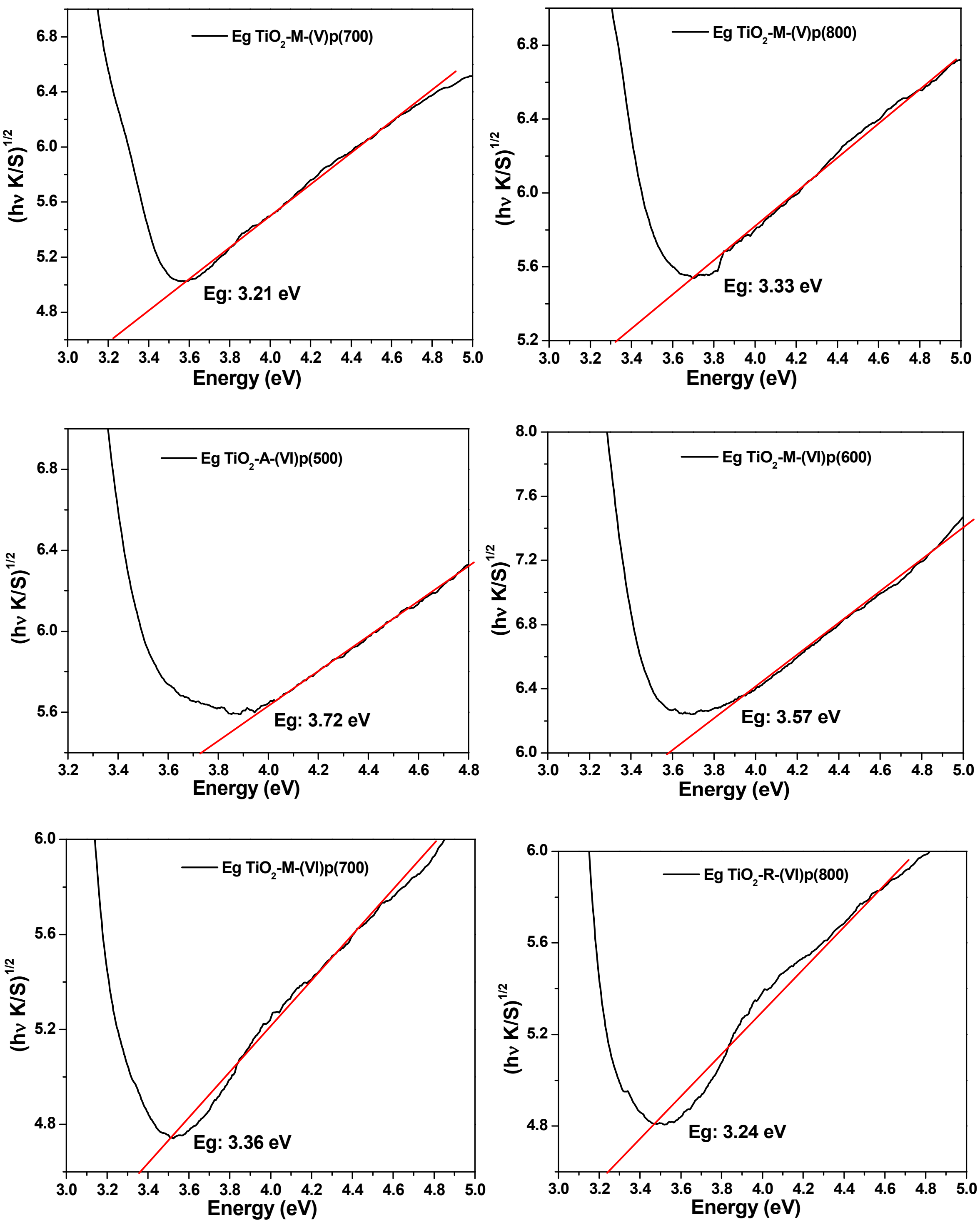

Figure S7. Tauc diagram from different TiO_2 nanostructures.

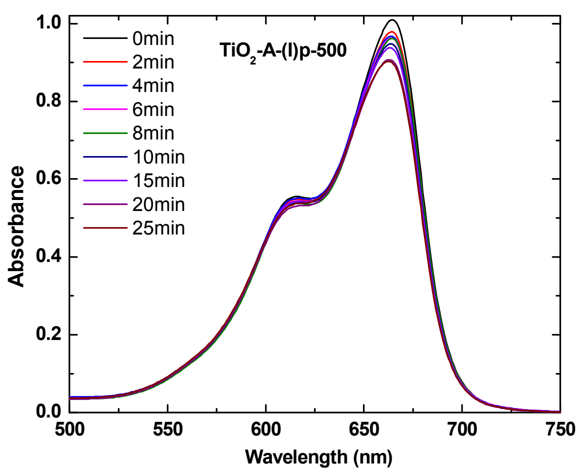
TiO2-A-(I)p-500
0min
2min
4min
6min
8min
10min
15min
20min
25min
Absorbance
Wavelength (nm)

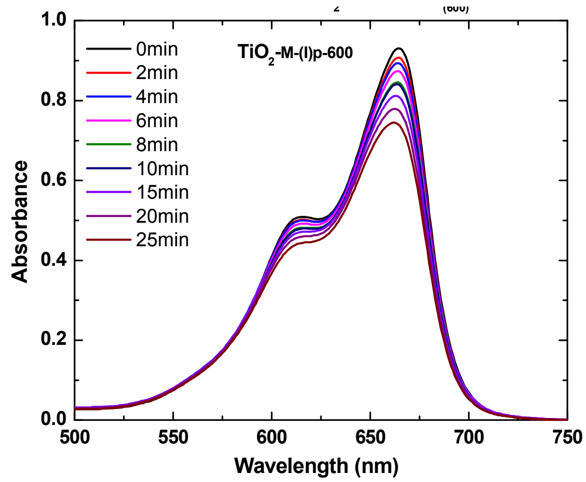
TiO2-M-(I)p-600
0min
2min
4min
6min
8min
10min
15min
20min
25min
Absorbance
Wavelength (nm)

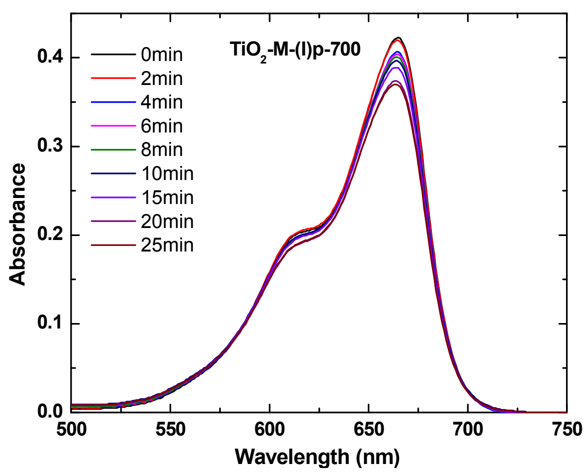
TiO2-M-(I)p-700
0min
2min
4min
6min
8min
10min
15min
20min
25min
Absorbance
Wavelength (nm)

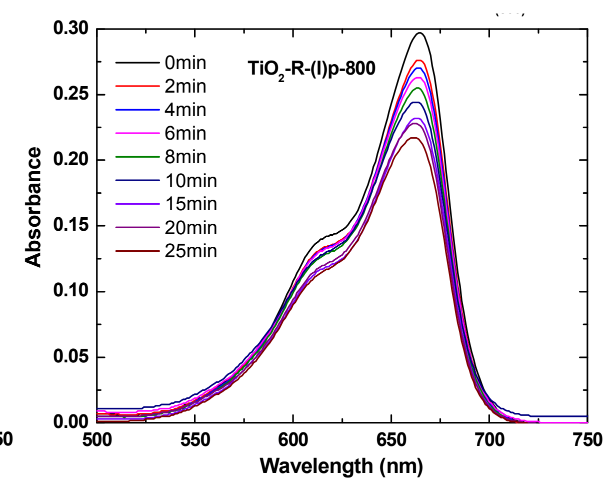
TiO2-R-(I)p-800
0min
2min
4min
6min
8min
10min
15min
20min
25min
Absorbance
Wavelength (nm)

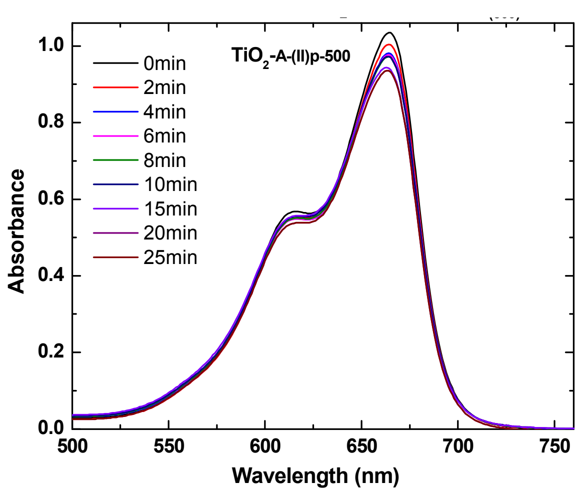
TiO2-A-(II)p-500
0min
2min
4min
6min
8min
10min
15min
20min
25min
Absorbance
Wavelength (nm)

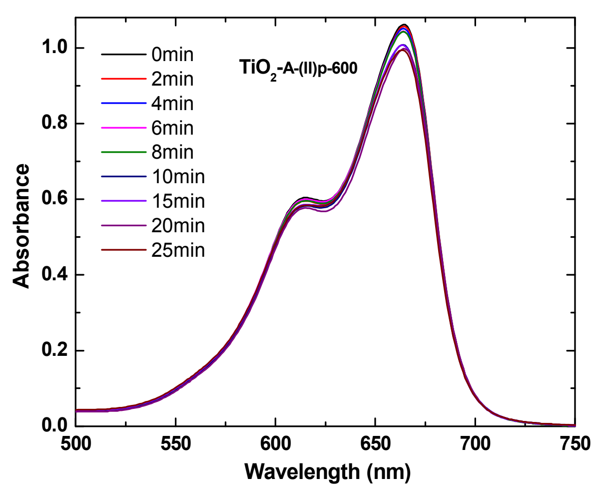
TiO2-A-(II)p-600
0min
2min
4min
6min
8min
10min
15min
20min
25min
Absorbance
Wavelength (nm)

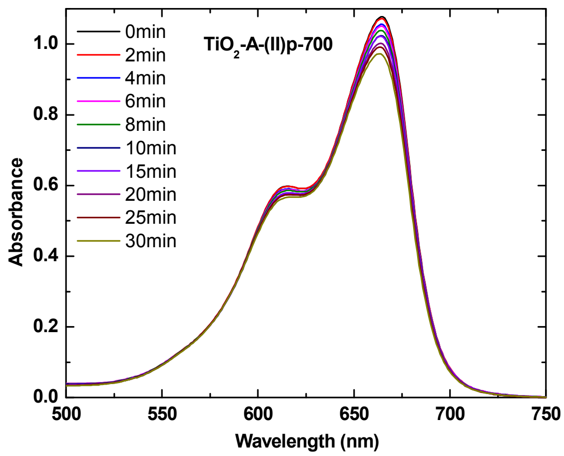
TiO$_2$-A-(II)p-700
0min
2min
4min
6min
8min
10min
15min
20min
25min
30min
Absorbance
Wavelength (nm)

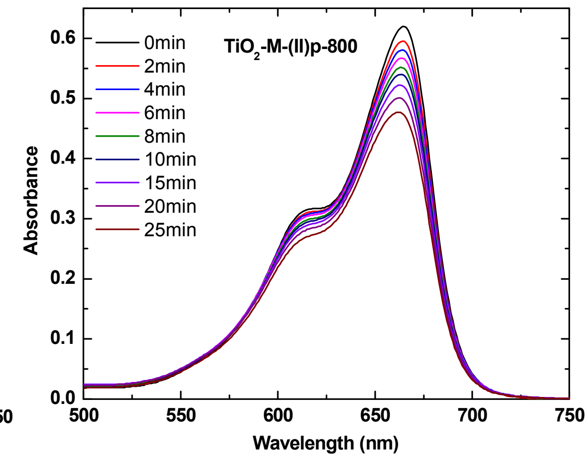
TiO$_2$-M-(II)p-800
0min
2min
4min
6min
8min
10min
15min
20min
25min
Absorbance
Wavelength (nm)

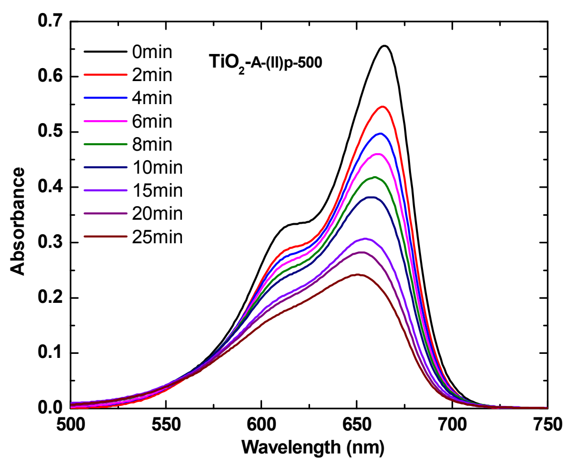
TiO$_2$-A-(II)p-500
0min
2min
4min
6min
8min
10min
15min
20min
25min
Absorbance
Wavelength (nm)

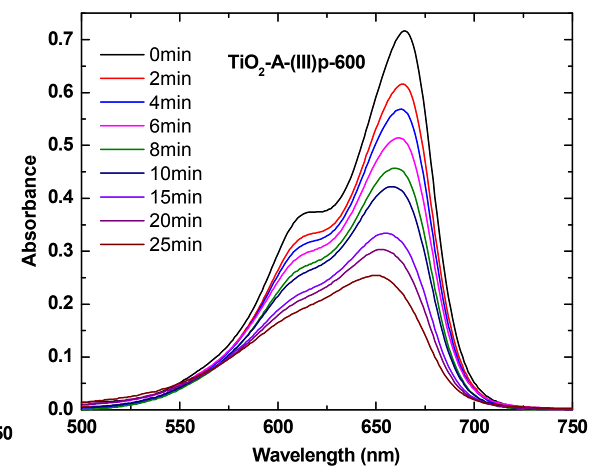
TiO$_2$-A-(III)p-600
0min
2min
4min
6min
8min
10min
15min
20min
25min
Absorbance
Wavelength (nm)

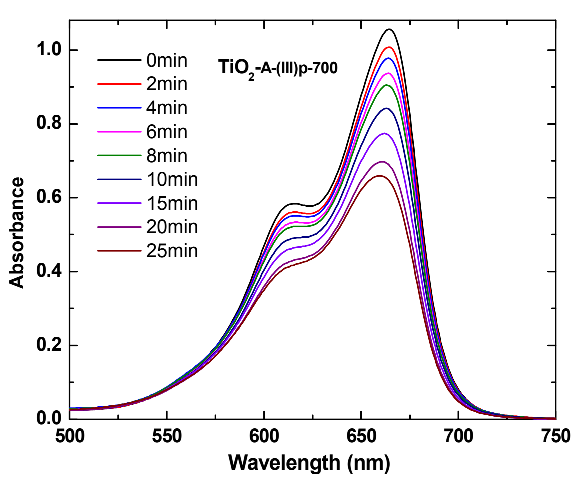
TiO$_2$-A-(III)p-700
0min
2min
4min
6min
8min
10min
15min
20min
25min
Absorbance
Wavelength (nm)

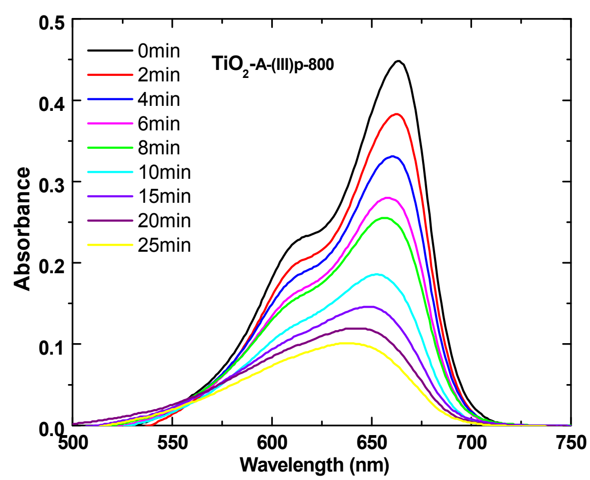
TiO$_2$-A-(III)p-800
0min
2min
4min
6min
8min
10min
15min
20min
25min
Absorbance
Wavelength (nm)

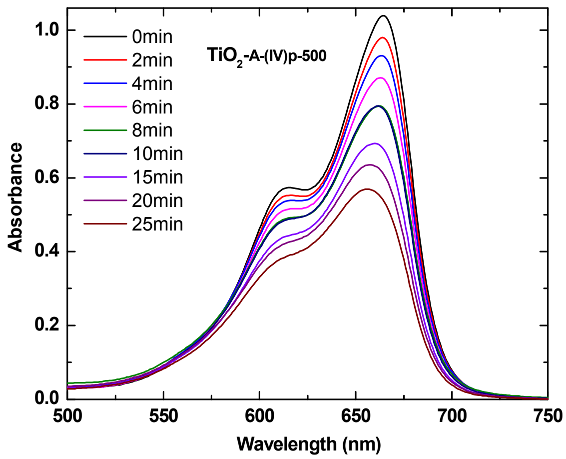

TiO2-A-(IV)p-500
0min
2min
4min
6min
8min
10min
15min
20min
25min
Absorbance
Wavelength (nm)

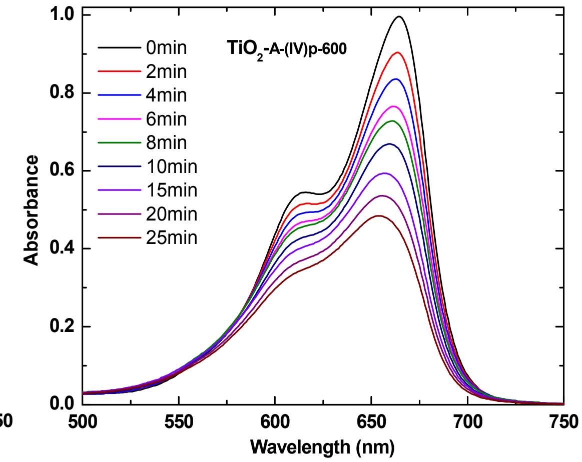

TiO2-A-(IV)p-600
0min
2min
4min
6min
8min
10min
15min
20min
25min
Absorbance
Wavelength (nm)

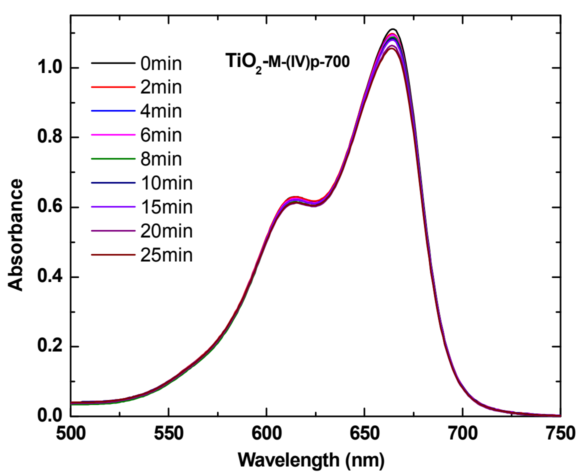

TiO2-M-(IV)p-700
0min
2min
4min
6min
8min
10min
15min
20min
25min
Absorbance
Wavelength (nm)

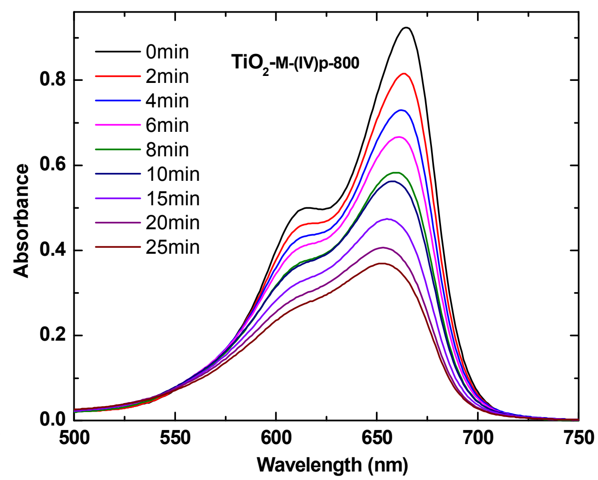

TiO2-M-(IV)p-800
0min
2min
4min
6min
8min
10min
15min
20min
25min
Absorbance
Wavelength (nm)

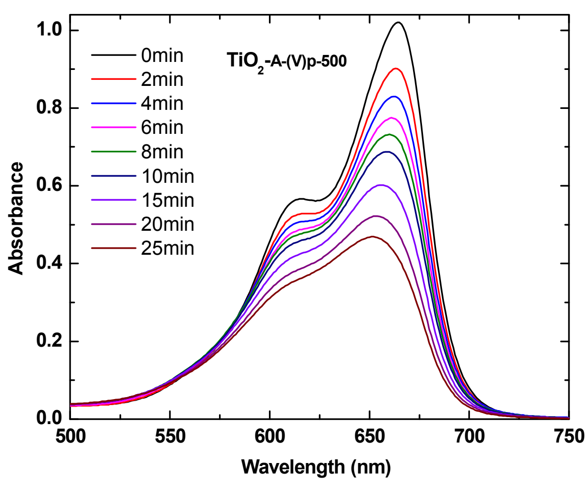

TiO2-A-(V)p-500
0min
2min
4min
6min
8min
10min
15min
20min
25min
Absorbance
Wavelength (nm)

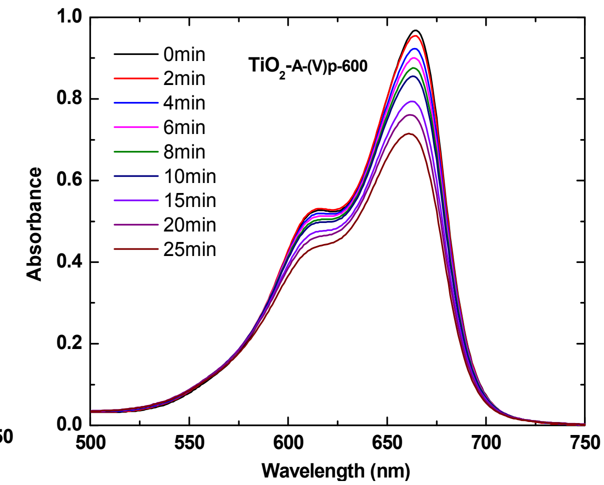

TiO2-A-(V)p-600
0min
2min
4min
6min
8min
10min
15min
20min
25min
Absorbance
Wavelength (nm)

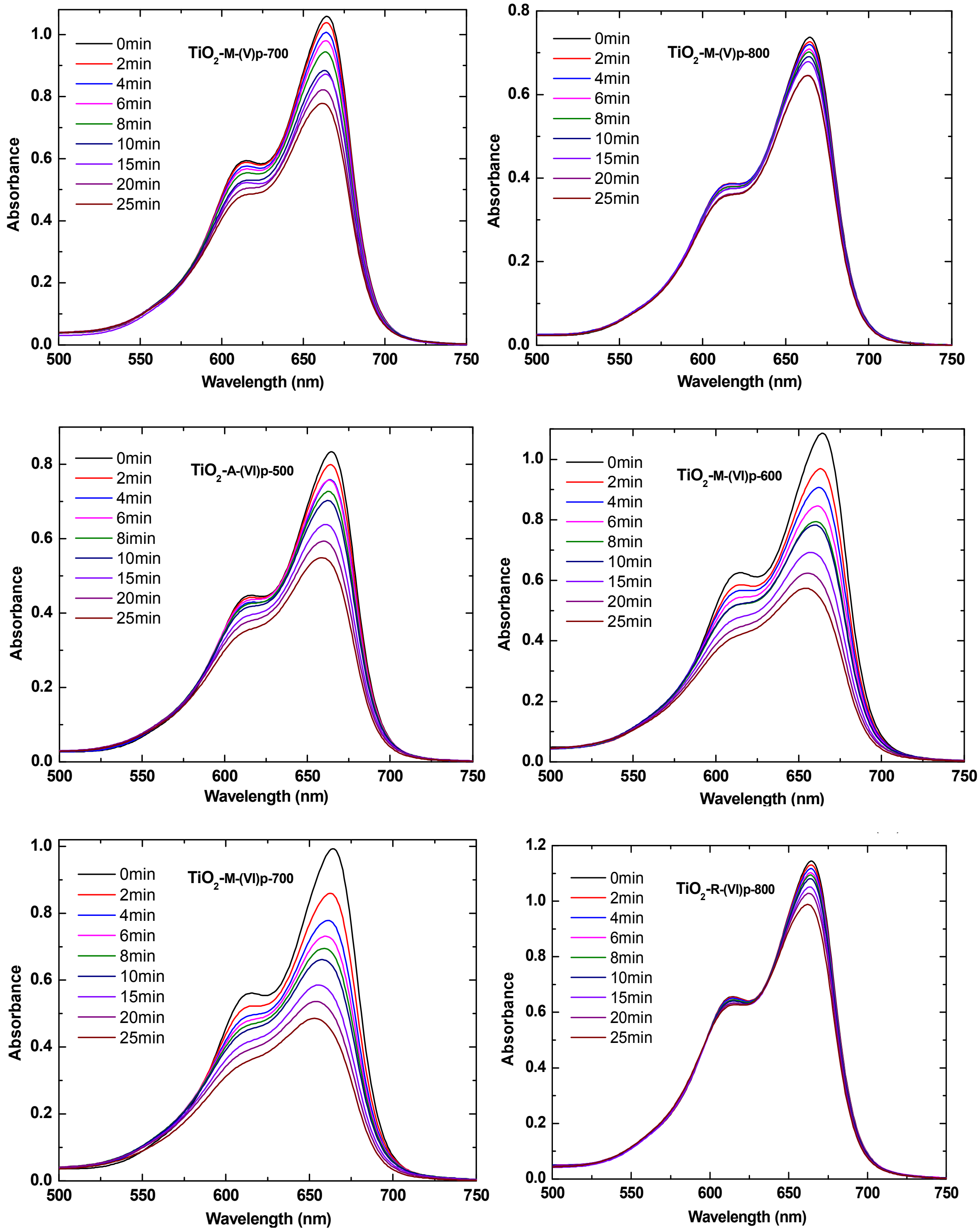

Figure S8. Degradation curves of MB in presence of all TiO_2 nanostructures.

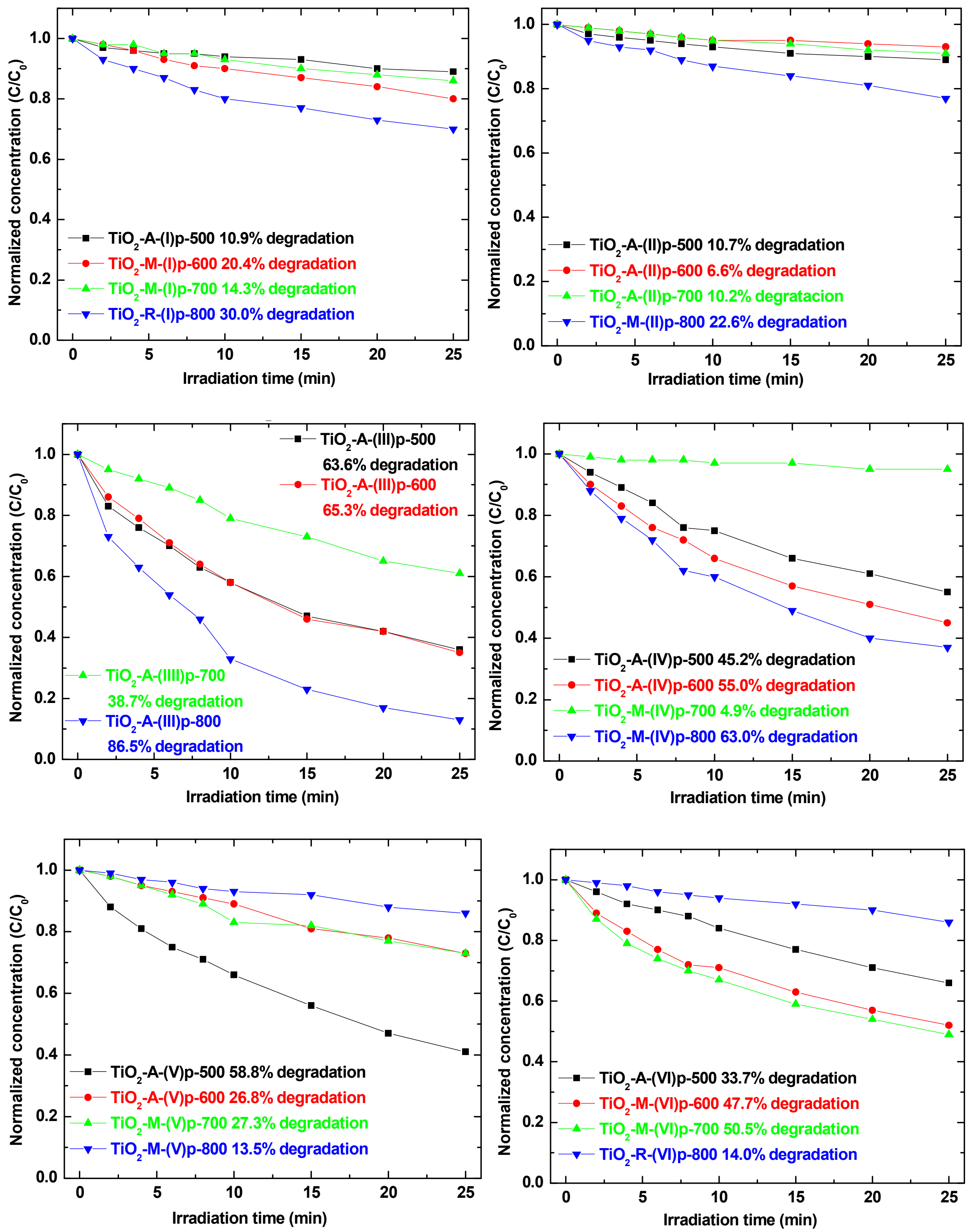

Figure S9. Normalized concentration changing of MB as a function of time for all TiO_2 photocatalyst obtained by precursors (I)p-(VI)p at different temperatures.

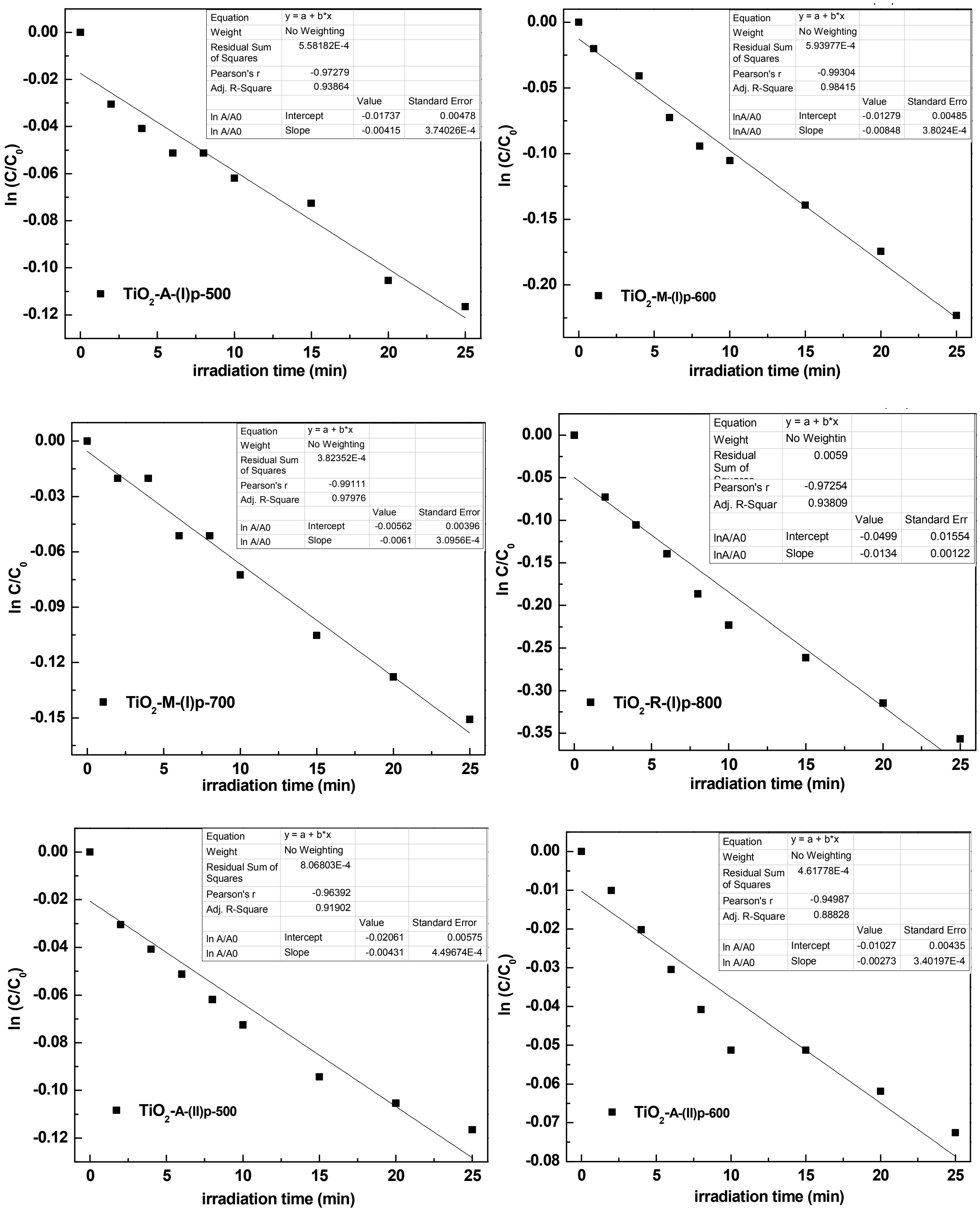

Equation y = a + b*x
Weight No Weighting
Residual Sum of Squares 5.58182E-4
Pearson's r -0.97279
Adj. R-Square 0.93864
Value Standard Error
ln A/A0 Intercept -0.01737 0.00478
ln A/A0 Slope -0.00415 3.74026E-4
TiO2-A-(I)p-500
ln (C/C0)
irradiation time (min)
Equation y = a + b*x
Weight No Weighting
Residual Sum of Squares 5.93977E-4
Pearson's r -0.99304
Adj. R-Square 0.98415
Value Standard Erro
lnA/A0 Intercept -0.01279 0.00485
lnA/A0 Slope -0.00848 3.8024E-4
TiO2-M-(I)p-600
ln (C/C0)
irradiation time (min)
Equation y = a + b*x
Weight No Weighting
Residual Sum of Squares 3.82352E-4
Pearson's r -0.99111
Adj. R-Square 0.97976
Value Standard Error
ln A/A0 Intercept -0.00562 0.00396
ln A/A0 Slope -0.0061 3.0956E-4
TiO2-M-(I)p-700
ln C/C0
irradiation time (min)
Equation y = a + b*x
Weight No Weightin
Residual Sum of 0.0059
Pearson's r -0.97254
Adj. R-Squar 0.93809
Value Standard Err
lnA/A0 Intercept -0.0499 0.01554
lnA/A0 Slope -0.0134 0.00122
TiO2-R-(I)p-800
ln C/C0
irradiation time (min)
Equation y = a + b*x
Weight No Weighting
Residual Sum of Squares 8.06803E-4
Pearson's r -0.96392
Adj. R-Square 0.91902
Value Standard Error
ln A/A0 Intercept -0.02061 0.00575
ln A/A0 Slope -0.00431 4.49674E-4
TiO2-A-(II)p-500
ln (C/C0)
irradiation time (min)
Equation y = a + b*x
Weight No Weighting
Residual Sum of Squares 4.61778E-4
Pearson's r -0.94987
Adj. R-Square 0.88828
Value Standard Erro
ln A/A0 Intercept -0.01027 0.00435
ln A/A0 Slope -0.00273 3.40197E-4
TiO2-A-(II)p-600
ln (C/C0)
irradiation time (min)

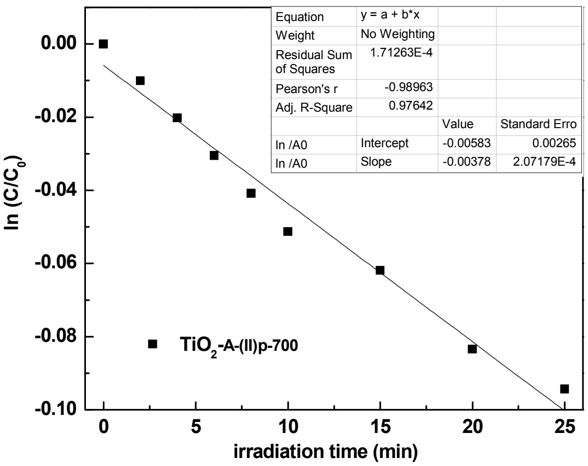
Equation y = a + b*x
Weight No Weighting
Residual Sum of Squares 1.71263E-4
Pearson's r -0.98963
Adj. R-Square 0.97642
Value Standard Erro
ln /A0 Intercept -0.00583 0.00265
ln /A0 Slope -0.00378 2.07179E-4
TiO2-A-(II)p-700
ln (C/C0)
irradiation time (min)

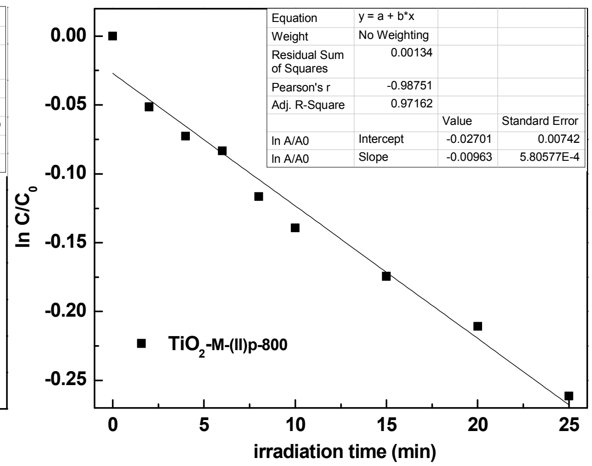
Equation y = a + b*x
Weight No Weighting
Residual Sum of Squares 0.00134
Pearson's r -0.98751
Adj. R-Square 0.97162
Value Standard Error
ln A/A0 Intercept -0.02701 0.00742
ln A/A0 Slope -0.00963 5.80577E-4
TiO2-M-(II)p-800
ln C/C0
irradiation time (min)

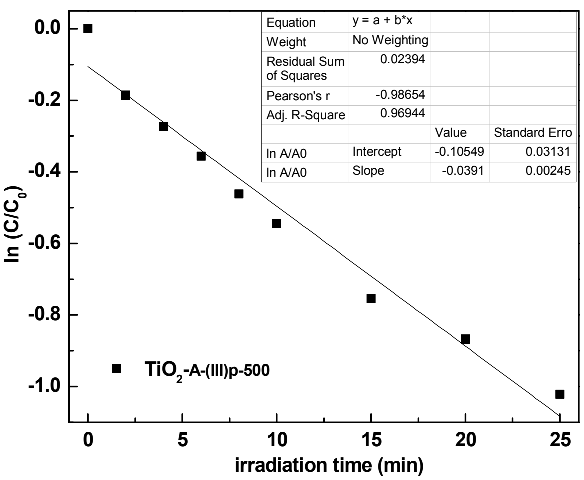
Equation y = a + b*x
Weight No Weighting
Residual Sum of Squares 0.02394
Pearson's r -0.98654
Adj. R-Square 0.96944
Value Standard Erro
ln A/A0 Intercept -0.10549 0.03131
ln A/A0 Slope -0.0391 0.00245
TiO2-A-(III)p-500
ln (C/C0)
irradiation time (min)

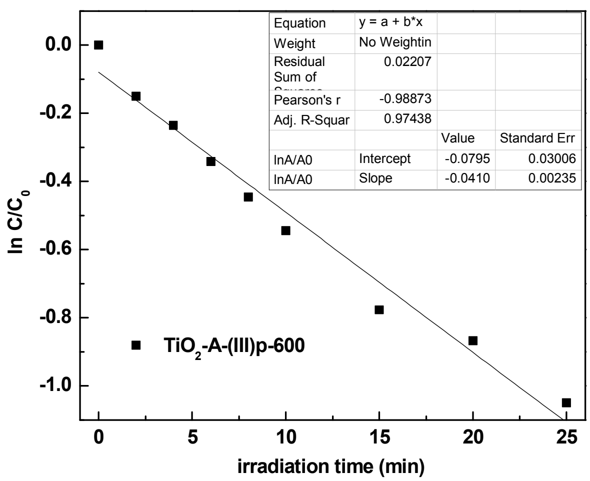
Equation y = a + b*x
Weight No Weightin
Residual Sum of
Pearson's r -0.98873
Adj. R-Squar 0.97438
Value Standard Err
lnA/A0 Intercept -0.0795 0.03006
lnA/A0 Slope -0.0410 0.00235
0.02207
TiO2-A-(III)p-600
ln C/C0
irradiation time (min)

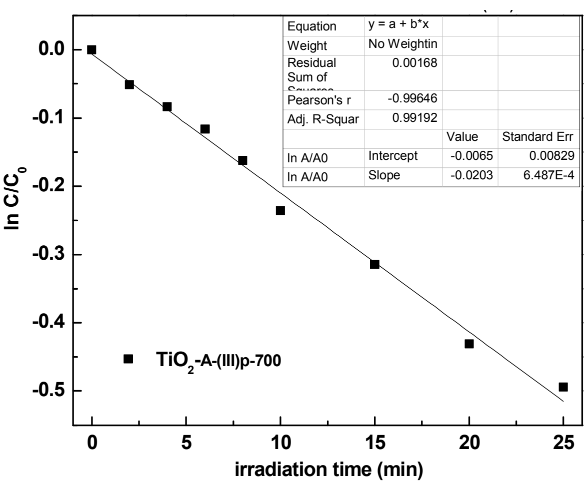
Equation y = a + b*x
Weight No Weightin
Residual Sum of 0.00168
Pearson's r -0.99646
Adj. R-Squar 0.99192
Value Standard Err
ln A/A0 Intercept -0.0065 0.00829
ln A/A0 Slope -0.0203 6.487E-4
TiO2-A-(III)p-700
ln C/C0
irradiation time (min)

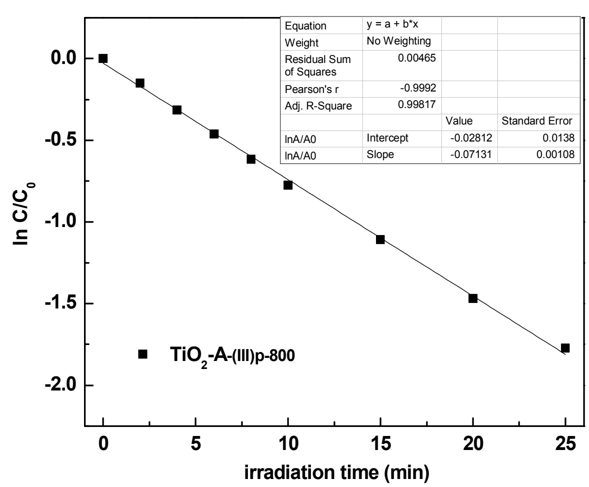
Equation y = a + b*x
Weight No Weighting
Residual Sum of Squares 0.00465
Pearson's r -0.9992
Adj. R-Square 0.99817
Value Standard Error
lnA/A0 Intercept -0.02812 0.0138
lnA/A0 Slope -0.07131 0.00108
TiO2-A-(III)p-800
ln C/C0
irradiation time (min)

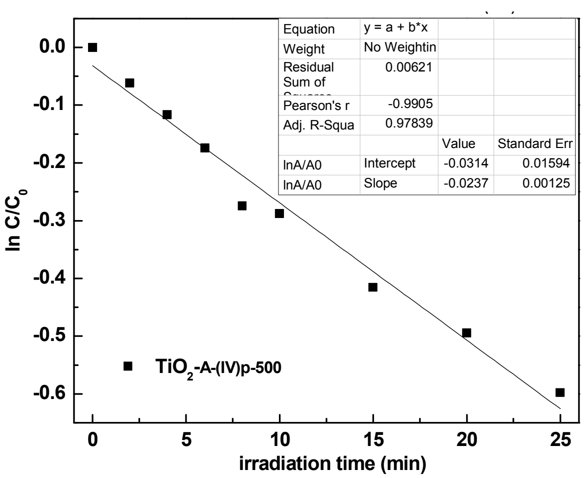
Equation y = a + b*x
Weight No Weightin
Residual Sum of 0.00621
Pearson's r -0.9905
Adj. R-Squa 0.97839
Value Standard Err
lnA/A0 Intercept -0.0314 0.01594
lnA/A0 Slope -0.0237 0.00125
TiO2-A-(IV)p-500
ln C/C0
irradiation time (min)

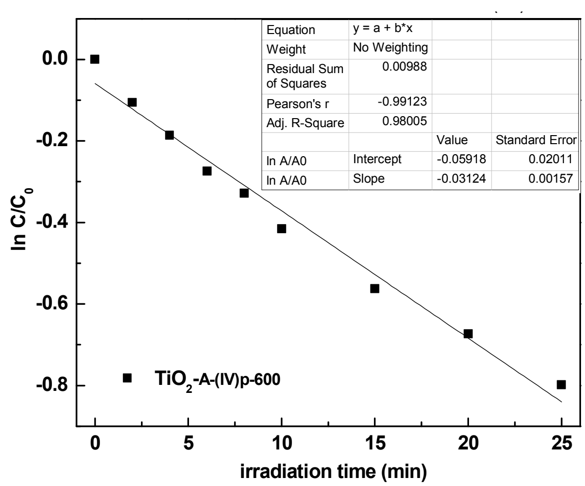
Equation y = a + b*x
Weight No Weighting
Residual Sum of Squares 0.00988
Pearson's r -0.99123
Adj. R-Square 0.98005
Value Standard Error
ln A/A0 Intercept -0.05918 0.02011
ln A/A0 Slope -0.03124 0.00157
TiO2-A-(IV)p-600
ln C/C0
irradiation time (min)

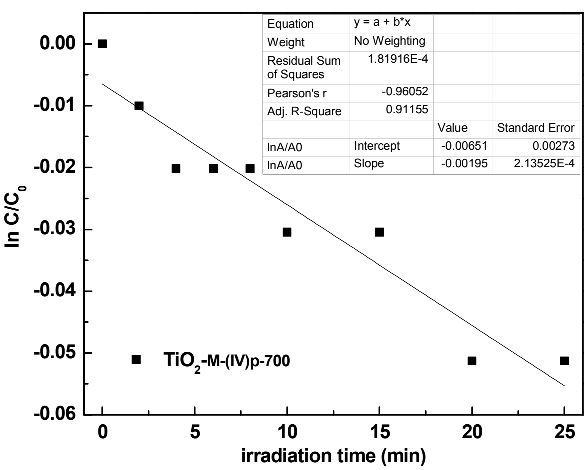
Equation y = a + b*x
Weight No Weighting
Residual Sum of Squares 1.81916E-4
Pearson's r -0.96052
Adj. R-Square 0.91155
Value Standard Error
lnA/A0 Intercept -0.00651 0.00273
lnA/A0 Slope -0.00195 2.13525E-4
TiO2-M-(IV)p-700
ln C/C0
irradiation time (min)

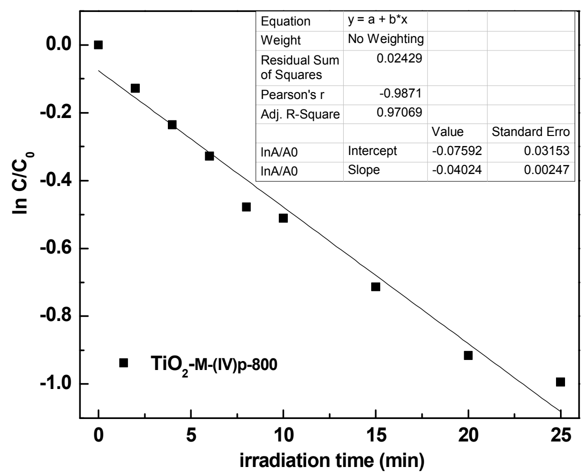
Equation y = a + b*x
Weight No Weighting
Residual Sum of Squares 0.02429
Pearson's r -0.9871
Adj. R-Square 0.97069
Value Standard Erro
lnA/A0 Intercept -0.07592 0.03153
lnA/A0 Slope -0.04024 0.00247
TiO2-M-(IV)p-800
ln C/C0
irradiation time (min)

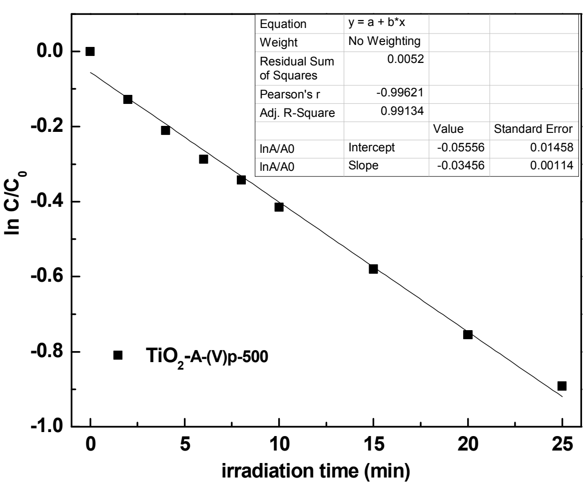
Equation y = a + b*x
Weight No Weighting
Residual Sum of Squares 0.0052
Pearson's r -0.99621
Adj. R-Square 0.99134
Value Standard Error
lnA/A0 Intercept -0.05556 0.01458
lnA/A0 Slope -0.03456 0.00114
TiO2-A-(V)p-500
ln C/C0
irradiation time (min)

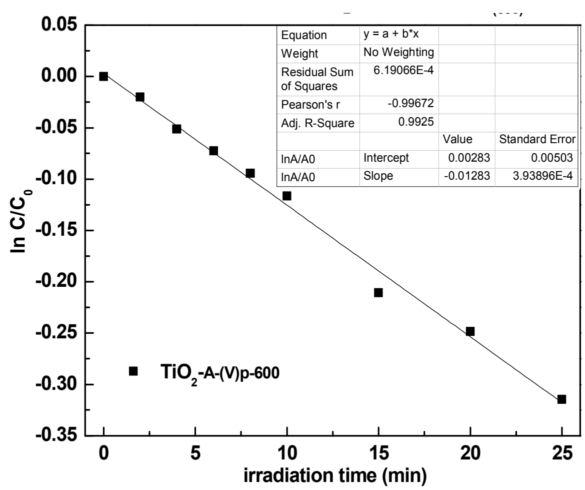
Equation y = a + b*x
Weight No Weighting
Residual Sum of Squares 6.19066E-4
Pearson's r -0.99672
Adj. R-Square 0.9925
Value Standard Error
lnA/A0 Intercept 0.00283 0.00503
lnA/A0 Slope -0.01283 3.93896E-4
TiO2-A-(V)p-600
ln C/C0
irradiation time (min)

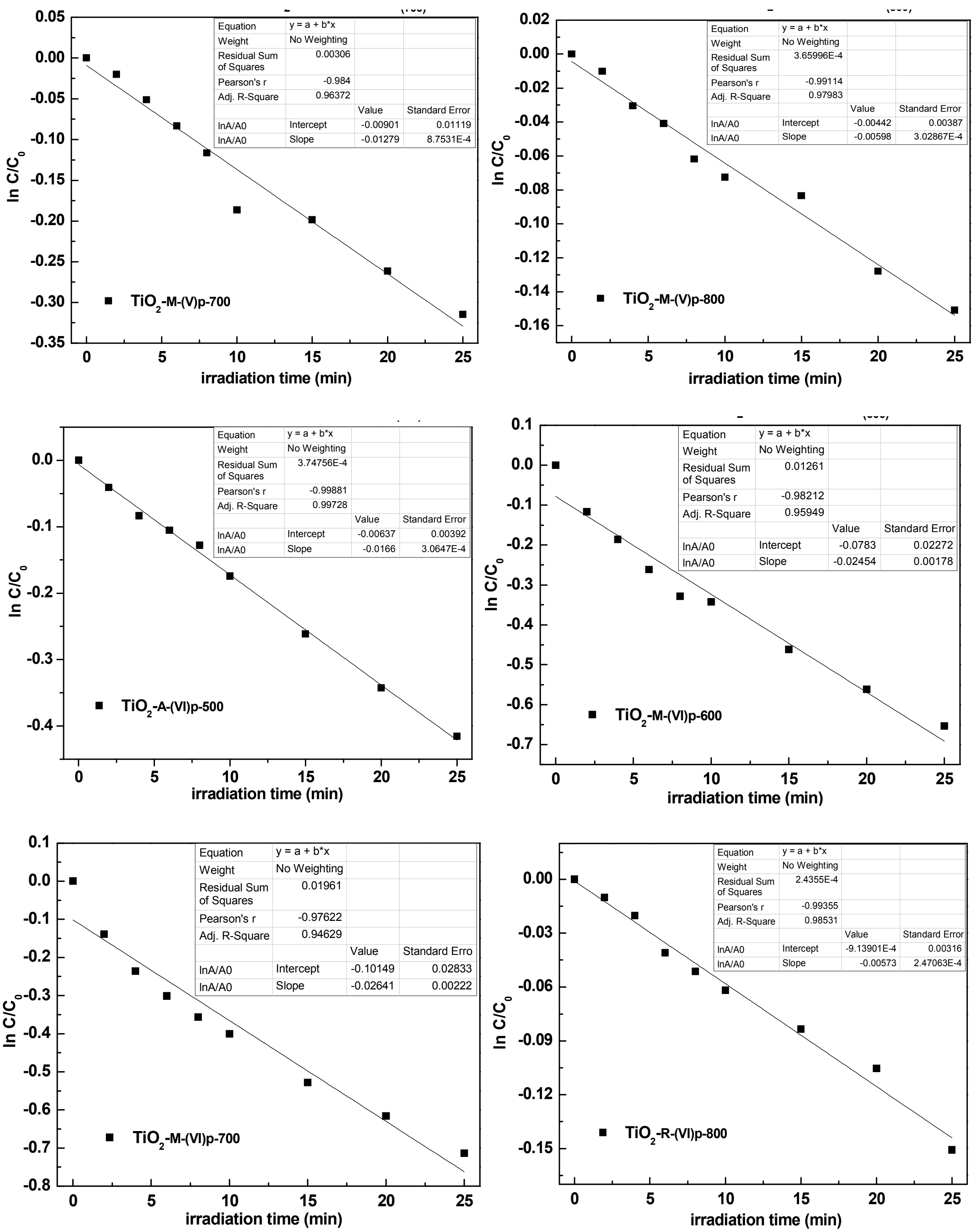

Figure S10. The pseudo-first-order kinetic of photocatalytic reactions for MB degradation process using different TiO_2 nanostructures.

Principal Component Analysis: phase. size. morphology

```
Analysis of the values and eigenvectors of the correlation matrix

Valor propio  1,6687  0,8652  0,4662
Proporción     0,556   0,288   0,155
Acumulada      0,556   0,845   1,000

              Phase   size morphology
Variable        PC1     PC2     PC3
phase        0,573  -0,591   0,568
size         0,665  -0,070  -0,744
morphology   0,479   0,803   0,353
```

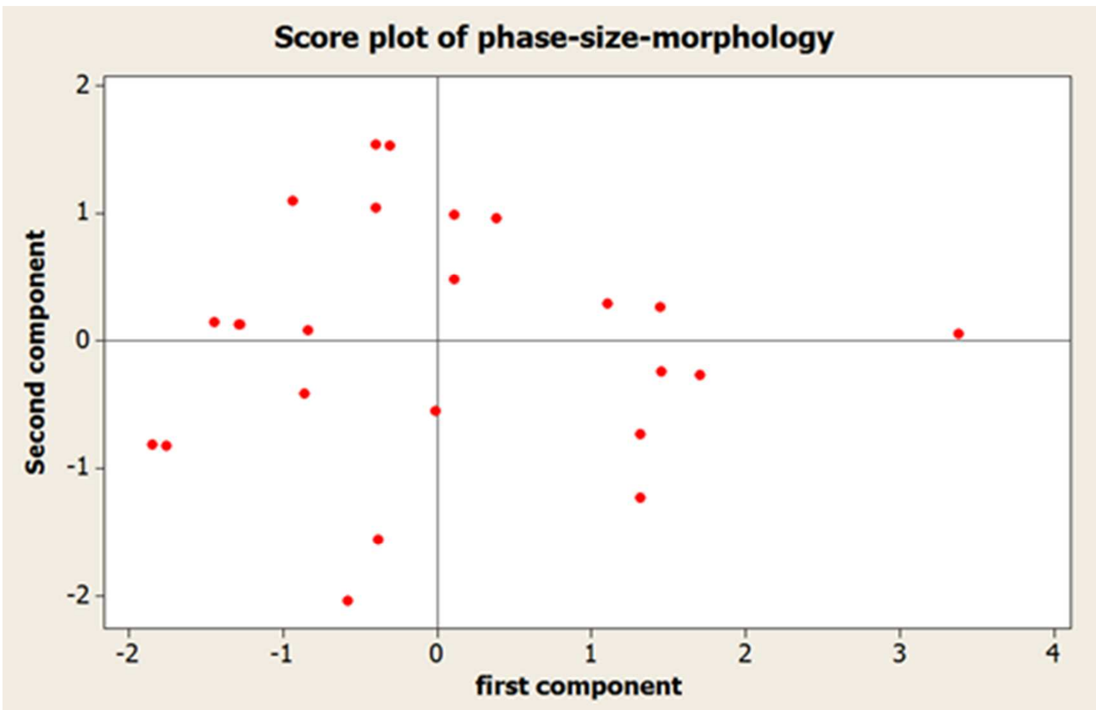

Figure S11. Statistical study using Principal Component Analysis of the three factors

Table S1. Anatase/rutile quantification for the pyrolytic precursors at several temperatures where the mixture was observed.

Pyrolytic precursors	Temperature (°C)	% ANATASE	% RUTILE
TiO_2-M-(I)p	600	88.10	11.9
TiO_2-M-(I)p	700	82.76	17.24
TiO_2-M-(II)p	800	64.01	35.99
TiO_2-M- IV)p	700	77.97	22.03
TiO_2-M- IV)p	800	68.35	31.65
TiO_2-M-(V)p	700	54.94	45.06
TiO_2-M-(V)p	800	63.41	36.59
TiO_2-M-(VI)p	600	93.79	6.21
TiO_2-M-(VI)p	700	34.00	66.00

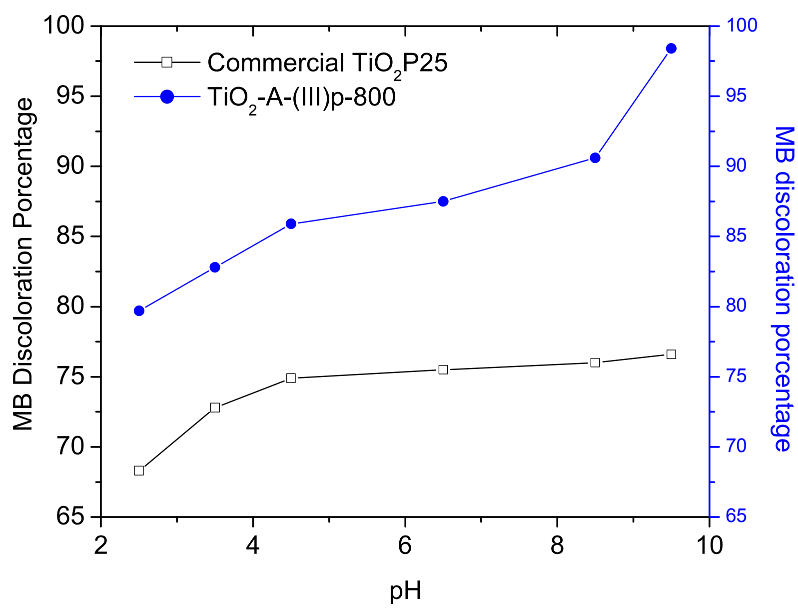

Figure S12. Effect of pH on MB ($1X10^{-5}$M) discoloration using our best TiO_2 photocatalyst and TiO_2 P25